

Feature functional theory - binding predictor (FFT-BP) for the blind prediction of binding free energies

Bao Wang^{1*}, Zhixiong Zhao^{2†}, Duc D. Nguyen¹ and Guo-Wei Wei^{1,3,4 ‡}

¹Department of Mathematics

Michigan State University, MI 48824, USA

²School of Medicine, Foshan University, Foshan, Guangdong 528000, China

³Department of Electrical and Computer Engineering

Michigan State University, MI 48824, USA

⁴Department of Biochemistry and Molecular Biology

Michigan State University, MI 48824, USA

August 26, 2018

Abstract

We present a feature functional theory - binding predictor (FFT-BP) for the protein-ligand binding affinity prediction. The underpinning assumptions of FFT-BP are as follows: i) representability: there exists a microscopic feature vector that can uniquely characterize and distinguish one protein-ligand complex from another; ii) feature-function relationship: the macroscopic features, including binding free energy, of a complex is a functional of microscopic feature vectors; and iii) similarity: molecules with similar microscopic features have similar macroscopic features, such as binding affinity. Physical models, such as implicit solvent models and quantum theory, are utilized to extract microscopic features, while machine learning algorithms are employed to rank the similarity among protein-ligand complexes. A large variety of numerical validations and tests confirms the accuracy and robustness of the proposed FFT-BP model. The root mean square errors (RMSEs) of FFT-BP blind predictions of a benchmark set of 100 complexes, the PDBBind v2007 core set of 195 complexes and the PDBBind v2015 core set of 195 complexes are 1.99, 2.02 and 1.92 kcal/mol, respectively. Their corresponding Pearson correlation coefficients are 0.75, 0.80, and 0.78, respectively.

Keywords: protein-ligand binding, scoring function, implicit solvent model, microscopic feature.

*Current address: Box 951555 Los Angeles, CA 90095-1555.

†The first two authors contribute equally to this work.

‡Correspondences should be addressed to Guo-Wei Wei. E-mail: wei@math.msu.edu.

Contents

I	Introduction	4
II	Theory and algorithm	6
II.A	Basic assumptions	6
	Representability assumption	6
	Feature-function relationship assumption	6
	Similarity assumption	6
II.B	Microscopic features	7
	Reaction field features	7
	Electrostatic binding features	8
	Atomic Coulombic interaction	8
	Atomic van der Waals interaction	8
	Atomic solvent excluded surface area and molecular volume	8
	Summary of microscopic features	8
II.C	Machine learning algorithm	10
II.D	Method for binding affinity prediction	10
III	Numerical results	11
III.A	Dataset preparation	12
	III.A.1 Datasets	12
	Validation set ($N = 1322$)	12
	Training sets	12
	Test sets	12
	III.A.2 Data pre-processing	12
III.B	Validation	12
	III.B.1 Validation on the validation set ($N = 1322$)	14
	III.B.2 Validation on the training set ($N = 3589$)	15
III.C	Blind predictions on three test sets	16
	III.C.1 Prediction on the benchmark set ($N = 100$)	16
	III.C.2 Prediction on the PDBBind v2007 core set ($N = 195$)	17
	III.C.3 Prediction on the PDBBind v2015 core set ($N = 195$)	18
IV	Concluding remarks	19

Table 1: List of abbreviations and symbols

Sign	Description
BRT	Boosted regression trees
CAAD	Computer aided drug design
EM	expectation-maximization algorithm
ESES	Eulerian solvent excluded surface software
FFT	Feature functional theory ⁱ
FFT-BP	Feature functional theory - binding predictor
GA	Genetic algorithm
GBDT	Gradient boosting decision tree
KECSA	Knowledge-based and empirical combined scoring algorithm
kNN	k-nearest neighbours
LJ	Lennard Jones
LTR	Learn to rank
MARS	Multivariate adaptive regression
MART	Multiple additive regression tree
MC	Monte Carlo
MD	Molecular dynamics
MIBPB	Matched interface and boundary-based Poisson-Boltzmann equation solver
MLR	Multiple linear regression
MM GBSA	Molecular mechanics generalized-Born surface area
MM PBSA	Molecular mechanics Poisson-Boltzmann surface area
PB	Poisson-Boltzmann
PMF	Potential of the mean force
QM/MM	Quantum mechanics/molecular mechanics
QSAR	Quantitative structure-activity relation
RF	Random forest
RMSE	Root mean square error
SPT	Scaled-particle theory
SVR	Support vector regression
vdW	van der Waals
VS	Virtual screening
[*]	Jump of quantity * across the interface Γ
$\ \mathbf{r}_i - \mathbf{r}_j\ $	Distance between two points located at \mathbf{r}_i and \mathbf{r}_j
Γ	Solvent-solute interface
ΔE_{MM}	Molecular mechanics energy
ΔG	Binding free energy
ΔG_{AB}	Binding free energy of molecular complex AB
ΔG_i	Binding free energy for i th complex
ΔG_{el}	Electrostatics binding free energy between protein and ligand
ΔG_{Coul}	Coulombic interaction
ΔG_{RF}	Reaction field energy
ΔG_{RF_i}	Atomic reaction field for i th atom
$(\Delta G_{RF})_{Com}$	Reaction field energy of complex
$(\Delta G_{RF})_{Lig}$	Reaction field energy of ligand
$(\Delta G_{RF})_{Pro}$	Reaction field energy of protein
ΔG_{solv}	Solvation free energy
$\delta(\mathbf{r} - \mathbf{r}_i)$	Delta function at point \mathbf{r}_i
ϕ	Electrostatics potential
ϕ_h	Electrostatics potential in homogeneous environment
ϕ_n	Normal derivative of function $\phi(\mathbf{r})$
$\epsilon(\mathbf{r})$	permittivity function
ϵ_{ij}	Measurement of the depth of the attractive well in van der Waals interaction u_{ij}
ϵ_m	Dielectric value of solute domain
ϵ_s	Dielectric value of solvent domain
Ω	$\Omega^m \cup \Omega^s$
Ω^m	Solute domain
Ω^s	Solvent domain

ⁱPlease do not confuse with fast Fourier transform.

Table 1 – continued

Sign	Description
f_{binding}	Unknown functional for modelling the relationship between binding free energy and extended features
f_j	unknown function modeling the j th physical observable of molecule A
N_m	Number of atoms in molecule
\mathbf{o}_{Aj}	j th physical observable \mathbf{o}_j of target molecule A
\mathbf{o}_{ij}	j macroscopic feature for i th molecule or complex
\mathbf{o}_i	Macroscopic feature vector for i th molecule or complex
Q_i	Partial charge located at \mathbf{r}_i
\mathbf{r}	Vector in \mathbf{R}^3
\mathbf{r}_i	3D coordinate of i th atom
r_i	Atomic radius of the i th atom
r_{ij}	Distance between two points located at \mathbf{r}_i and \mathbf{r}_j
$T\Delta S$	Entropy
u_{ij}	van der Waals interaction between i th and j th atoms
\mathbf{v}_i	Extended feature vector $\mathbf{v}_i = (\mathbf{x}_i, \mathbf{o}_i)$ for i th molecule or complex
\mathbf{x}_A	Microscopic feature vector of the target molecule A
\mathbf{x}_{AB}	Microscopic feature vector of the target complex AB
\mathbf{x}_i	Microscopic feature vector for i th molecule or complex
\mathbf{x}_{ij}	j th microscopic feature for i th molecule

I Introduction

Designing efficient drugs for curing diseases is of essential importance for the new century's life science. Indeed, one of the ultimate goals of molecular biology is to understand the molecular mechanism of human diseases and to develop efficient side-effect-free drugs for disease curing. Nevertheless, the drug discovery procedure is extremely complicated, and involves many scientific disciplines and technologies. As a brief summary, the drug discovering contains the following seven major steps,⁸ namely, i) Disease identification; ii) Target hypothesis, i.e., the activation or inhibition of drug targets (usually proteins within the cell) is thought to alter the disease state; iii) Screening potential principle compounds that will bind to the target; iv) Optimizing the identified compounds with respect to their structural characteristics in the context of the target binding site; v) Preclinical test, both *in vitro* and *in vivo* tests will be performed; vi) Clinical trials to determine their bioavailability and therapeutic potential; and vii) Optimizing chemical's efficacy, toxicity, and pharmacokinetics properties. Typically, the whole cost of a new drug development is estimated to be more than one billion dollars with more than ten years' research efforts.⁹³ Such large amount of cost is mostly due to unsuitable chemical compounds that are used in the preclinical and clinical testing.² In terms of economical drug design, sophisticated and accurate computer aided compound screening methods become extremely important. Virtual screening (VS) methodologies focus on detecting a small set of highly promising candidates for further experimental testing.⁷¹ Docking is one of the most important VS methodologies and is widely used in the computer aided drug design (CADD). It is a two-stage protocol.⁶ The first step is the sampling of the ligand binding conformations, which determines the pose, orientation, and conformation of a molecule as docked to the target binding site.¹¹ The second stage is the scoring of protein-ligand binding affinity. With the development of molecular dynamics (MD), Monte Carlo (MC), and genetic algorithm (GA) for pose generation, the sampling problem is relatively well resolved.^{46,62,86} A major remaining challenge in achieving accurate docking is the development of accurate scoring functions for diverse protein ligand complexes. One of the most important open problems in computational biosciences is the accurate prediction of the binding affinities of a large set of diverse protein-ligand complexes.⁶ A desirable goal is to achieve less than 1 kcal/mol root mean square error (RMSE) in the prediction.

Since the pioneer work in the 1980s and 1990s, the study of the scoring function and sampling techniques has been blooming in the CADD community.^{20,31,40,44} In a recent review, Liu and Wang classify the existing popular scoring functions into four categories,⁵³ namely, i) Force-field based or physical based scoring functions; ii) Empirical or regression based scoring functions; iii) Potential of the mean force (PMF) or knowledge based scoring functions; and iv) Machine learning based scoring functions. Physics based scoring functions provide some of the most accurate and detailed description of the protein and ligand molecules in the solvent environment. Typical models that belong to this category are molecular mechanics Poisson-Boltzmann surface area (MM PBSA) and molecular mechanics generalized-Born surface area (MM GBSA)^{29,43} with a given force field parametrization of both solvent and solute molecules, like Amber or CHARMM force fields.^{56,84,89} In this framework, the binding free energy is often modeled as a superposition of four parts: van der Waals (vdW), electrostatics interactions between protein and ligand, the hydrogen bonding, and solvation effects. In addition to MM PBSA and MM GBSA, several other prestigious scoring functions also belong to this category, including COMBINE⁶⁴ and MedusaScore.⁹⁰ Physical based scoring functions are a class of dynamically improved methods and the VS can become more and more accurate with the further development of advanced and comprehensive molecular mechanics force fields. Plenty of improvement has already been done for improving the accuracy of scoring functions, such as QM/MM multiscale

coupling⁷⁵ and polarizable force fields.⁶⁶ Empirical or regression based scoring functions, usually also called multiple linear regression (MLR) scoring functions, typically model the protein-ligand binding affinity contributed from vdW interaction, hydrogen bonding, desolvation, and metal chelation.⁹⁴ Several parameters are introduced in each of the above term, and the scoring function is obtained by using the existing protein-ligand binding information to train these parameters in the given binding affinity function. Many other existing scoring functions also belong to this category, e.g., PLP,⁷⁹ ChemScore,²¹ and X-Score,⁸⁵ etc.

A recent study on a congeneric series of thrombin inhibitors concludes that free energy contributions to protein-ligand binding are non-additive, showing some theoretical deficiencies of the MLR based scoring functions.⁷ The theoretical basis of this non-additivity was explained in an earlier review.⁹⁷ Machine learning algorithms do not explicitly require a given form of the binding affinity to its related items, and thus do not require the additive assumption of energetic terms. Many machine learning based scoring functions are proposed in the past few decades. These methods apply quantitative structure-activity relation (QSAR) principles to the prediction of the protein-ligand binding affinity. Representative work along this line is the random forest (RF) based scoring function, RF-Score.⁴⁹ In RF-Score, the random forest is selected as the basic regressor instead of the classical MLR, which is restricted to the pre-defined linear form of the binding affinity function. By utilization of the features calculated from the existing scoring functions, it achieves highly accurate five-fold cross validation results on the PDBBind v2013 refined set. Prediction results on the PDBBind v2007 core set further confirms the accuracy of the RF-Score.⁴⁹ Many other machine learning tools are utilized as the main skeletons of the scoring functions, like support vector regression (SVR),⁴² multivariate adaptive regression (MARS), k-nearest neighbours (kNN), boosted regression trees (BRT), etc.³ The blooming of the big data approaches and more accurate descriptors characterization of the protein-ligand binding effects have made machine learning type of scoring functions full of vitality in CADD. Machine learning based scoring functions can make continuous improvement through both advance in physical protein-ligand binding descriptors and discovery of new machine learning techniques.

Another important class of scoring functions is PMF based. This category of scoring functions is based on the simplified statistical mechanics theory in which the protein ligand binding affinity is modeled as the sum of pairwise statistical potentials between protein and ligand atoms. The major merit of the PMF type of scoring functions is their simplicity in both concept and computation. This simplified physical model captures major physical principles behind the protein ligand binding. In knowledge-based and empirical combined scoring algorithm (KECSA), the binding affinity between protein and ligand are modeled by 49 pairwise modified Lennard-Jones types of potentials between different types of atoms.⁹⁵ Through a large number of training instances, the functional form of all these pairwise interaction potentials can be determined. Effective ligand binding conformation sampling procedure can also be incorporated into this theoretical framework.⁹⁶ There are also many other interesting developments in the PMF based scoring functions, e.g., PMF,⁶⁰ DrugScore,⁷⁸ and IT-Score.³⁴

Essentially, the major purpose of a scoring function is to find the relative order of binding affinities of candidate chemicals to the target binding site. This ranking result is further used for the preclinical test in a realistic drug design procedure. From this point of view, the development of scoring functions turns out to be the development of ranking methods. Many existing scoring functions have been developed from this perspective. For example, learning to rank (LTR) algorithms have been used to develop various scoring functions, including PTRank, RankNet, RankNet, RankBoost, ListNet, and AdaRank.^{2,81,87,93} Compared to other machine learning or simple MLR based scoring functions, the advantages of ranking based scoring functions are two-fold. First, they are applicable to identifying compounds on novel protein binding sites where no sufficient data available for other machine learning algorithms. Second, they are suitable for the case that binding affinities are measured in different platforms since ranking can be more focused on relative order.⁹³

In this work, we propose a feature functional theory-binding predictor (FFT-BP) for the blind prediction of binding affinity. The FFT-BP is constructed based on three assumptions, i.e., i) representability assumption: there exists a microscopic feature vector that can uniquely characterize and distinguish one molecular complex from another; ii) feature-function relationship assumption: the macroscopic features, including binding free energy, of a molecule or complex is a functional of microscopic feature vectors; and iii) similarity assumption: molecules or complexes with similar microscopic features have similar macroscopic features, such as binding free energies. FFT-BP has three distinguishing traits. A major trait of the proposed FFT-BP is its use of microscopic features derived from physical models, including Poisson Boltzmann (PB) theory,^{16,28,33,68,72,73,83} nonpolar solvation models,^{17,19,24,25,74,80,88} components in MM PBSA⁴³ and quantum models. As such, electrostatic solvation free energy, electrostatic binding affinity, atomic reaction field energies, and Coulombic interactions are utilized to represent the electrostatic effects of protein-ligand binding. Atomic pairwise van der Waals interactions are employed to model the dispersion interactions between the protein and ligand. We also make use of atomic surface areas and molecular volume in our FFT-BP to describe hydrophobic and entropy effects of the protein-ligand binding process. Another trait of the present FFT-BP is its feature-function relationship assumption, which avoids the use of additive modelling of the total binding affinity based on the direct sum of various energy components. Machine learning algorithms automatically rank the relative importance of various features to the binding affinity. By utilizing the boosted regression tree type of algorithms for the ranking, our model can capture the nonlinear dependence of the binding affinity to each feature. The other trait of FFT-BP is its use of advanced LTR algorithm, the multiple additive regression tree (MART), for ranking the nearest neighbors via microscopic features. This approach allows us to further improve our method by incorporating the state-of-the-art machine learning techniques.

This paper is structured as follows. In Section II, we present the theoretical background of FFT-BP, which consists of four

parts, basic assumptions, microscopic feature selection, MART algorithm and binding affinity function. In Section III, we verify the accuracy and robustness of our FFT-BP by a validation set, a training set and three standard test sets involving a variety of diverse protein-ligand complexes. We show that FFT-BP delivers some of the best binding affinity predictions. This paper ends with concluding remarks.

II Theory and algorithm

In this section, we present FFT for binding free energy prediction. First, we discuss the basic FFT assumptions. Additionally, feature selections are based on physical models. Moreover, protein-ligand complexes are ranked from a machine learning algorithms, i.e., the MART ranking algorithm. Finally, we describe a prediction algorithm for approximating the binding free energy based on features from nearest neighbors ranked by the MART algorithm.

II.A Basic assumptions

Our FFT is based on three assumptions, including representability, feature-functional relationship and similarity. These assumptions are described below.

Representability assumption Without loss of generality, we consider a total of N molecules or complexes $\{M_i\}_{i=1}^N$ with known names and geometric structures from related databases. One of FFT basic assumptions is that there exists an n -dimensional microscopic feature vector, denoted as $\mathbf{x}_i = (\mathbf{x}_{i1}, \mathbf{x}_{i2}, \dots, \mathbf{x}_{in})$ to uniquely characterize and distinguish the i th molecule or complex. Here the vector components include various microscopic features, such as atomic types and numbers, atomic charges, atomic dipoles, atomic quadrupole, atomic reaction field energies, electrostatic solvation or electrostatic binding free energies, atomic surface areas, pairwise atomic van der Waals interactions, etc.

For i th molecule or complex, apart from its n microscopic features, there are l macroscopic features, or physical observable $\mathbf{o}_i = (\mathbf{o}_{i1}, \mathbf{o}_{i2}, \dots, \mathbf{o}_{il})$, such as density, boiling point, enthalpy of formation, heat of combustion, solvation free energy, pKa, viscosity, permittivity, electrical conductivity, binding free energy, etc. We combine the microscopic and macroscopic feature vectors to construct an extended feature vector $\mathbf{v}_i = (\mathbf{x}_i, \mathbf{o}_i)$ for the i th molecule.

Extended feature vectors $\{\mathbf{v}_i\}_{i=1}^N$ span a vector space \mathcal{V} , which satisfies commonly required eight axioms for addition and multiplication, such as associativity, commutativity, identity element, and inverse elements of addition, compatibility of scalar multiplication with field multiplication, etc. Unlike the usual L_p space, the extended feature space does not have the notion of nearness, angles or distances. We therefore need additional techniques, namely, machine learning algorithms, to study the nearness and distance between feature vectors. The selection of microscopic features depends on what physical or chemical prediction is interested. In our approach, we utilize microscopic features from related physical models. For example, for solvation and binding free energy prediction, we select features that are derived from implicit solvent models and quantum mechanics.

Based on our assumption, microscopic features alone are able to characterize and distinguish molecules. In contrast, macroscopic features are used as the label in learning and ranking for a given purpose. Therefore, for a given task, say binding free energy prediction, we do not include all the macroscopic features in the feature vector \mathbf{o}_i . We only select $\mathbf{o}_i = (\mathbf{o}_{i1}) = \Delta G_i, \forall i = 1, \dots, N$, where $\{\Delta G_i\}$ are known binding free energies from databases. The resulting extended vector is used for the binding free energy prediction.

Feature-function relationship assumption In FFT, a general feature-function relationship is assumed for the j th physical observable \mathbf{o}_j of target molecule A

$$\mathbf{o}_{Aj} = f_j(\mathbf{x}_A, \mathbf{v}_1, \mathbf{v}_2, \dots, \mathbf{v}_N), \quad (1)$$

where f_j is an unknown function modeling the j th physical observable of molecule A and \mathbf{x}_A is the microscopic feature vector of the target molecule A. This relation applies to the prediction of various physical and chemical properties. In the present application, we are interested in the prediction of binding free energies for a set of diverse protein-ligand complexes. We construct a feature space for the training set and the binding free energy of target molecular complex AB can be given as a functional of extended feature vectors

$$\Delta G_{AB} = f_{\text{binding}}(\mathbf{x}_{AB}, \mathbf{v}_1, \mathbf{v}_2, \dots, \mathbf{v}_N) \quad (2)$$

where ΔG_{AB} is the binding free energy of molecular complex AB, and f_{binding} is an unknown functional for modeling the relationship between binding free energy and extended features. Obviously, the determination of f_{binding} is a major task of the present work.

Similarity assumption In the FFT, we assume that molecules with similar microscopic features have similar macroscopic features, or physical observables. In the present application, we assume that protein complexes with similar microscopic features will have similar binding free energies. This assumption provides the basis for utilizing supervised machine learning algorithms to rank protein-ligand complexes.

In our earlier HPK model, we assume that molecules with similar features have the same set of parameters in a physical model. As a result, solvation or binding free energies are still computed based on a physical model, while a machine learning algorithm is used to find out the nearest neighbors for modeling physical parameters. In the present FFT, the binding free energy is not modeled by a physical model directly. However, the microscopic features are constructed from physical models.

II.B Microscopic features

In physical models, such as MM PBSA and MM GBSA, the protein ligand binding affinity is given by the combination of molecular mechanics energy, solvation free energy, and entropy term

$$\Delta G = \Delta E_{\text{MM}} + \Delta G_{\text{solv}} - T\Delta S, \quad (3)$$

where ΔE_{MM} , ΔG_{solv} , and $T\Delta S$ are the molecular mechanics energy, solvation free energy, and entropy terms, respectively. Further, the molecular mechanics energy can be decomposed as E_{Covalent} , which is the sum of bond, angle, and torsion energy terms, and $E_{\text{Noncovalent}}$, which includes the van der Waals term and a Coulombic term E_{Coul} .³² Equation (3) is used as a guidance for the feature selection in our FFT-Score model.

Reaction field features Molecular electrostatics is of fundamental importance in the protein solvation and binding processes.^{28,33,73} In this work, we use a classical implicit solvent model, the PB theory, for modeling the molecular electrostatics in the solvent environment. This model is used for two purposes. On the one hand, the solvation effects during the protein ligand binding will be modeled via this theory. On the other hand, the electrostatic contribution to the protein ligand binding affinity is computed based on this model, as well.

For simplicity, we consider the linearized PB model in the pure water solvent, which is formulated as the following elliptic interface problem in mathematical terminology. The governing equation is given by

$$-\nabla \cdot (\epsilon(\mathbf{r})\nabla\phi(\mathbf{r})) = \sum_{i=1}^{N_m} Q_i\delta(\mathbf{r} - \mathbf{r}_i), \quad (4)$$

with the interface conditions

$$[\phi]|_{\Gamma} = 0, \quad (5)$$

and

$$[\epsilon\phi_{\mathbf{n}}]|_{\Gamma} = 0, \quad (6)$$

where ϕ is the electrostatics potential over the whole solvent solute domain, Q_i is the partial charge located at \mathbf{r}_i and $\delta(\mathbf{r} - \mathbf{r}_i)$ is the delta function at point \mathbf{r}_i . The permittivity function $\epsilon(\mathbf{r})$ is given by

$$\epsilon(\mathbf{r}) = \begin{cases} \epsilon_m = 1, & \mathbf{r} \in \Omega^m \\ \epsilon_s = 80, & \mathbf{r} \in \Omega^s \end{cases} \quad (7)$$

where Ω^m and Ω^s are solute and solvent domains, respectively. The two domains are separated by the molecular surface Γ .

The following Debye-Huckel type of boundary condition is imposed to make the PB model well posed

$$\phi(\mathbf{r}) = \sum_{i=1}^{N_m} \frac{Q_i}{4\pi\epsilon_s|\mathbf{r} - \mathbf{r}_i|}, \text{ if } \mathbf{r} \in \partial\Omega, \quad (8)$$

where $\Omega = \Omega^m \cup \Omega^s$.

Molecular reaction field energy is computed by the following formula

$$\Delta G_{\text{RF}} = \sum_{i=1}^{N_m} \Delta G_{\text{RF}i} \quad (9)$$

where the i th atomic reaction field energy $\Delta G_{\text{RF}i}$ is given by

$$\Delta G_{\text{RF}i} = \frac{1}{2}Q_i(\phi(\mathbf{r}_i) - \phi_h(\mathbf{r}_i)) \quad (10)$$

where ϕ_h is obtained through solving the PB model with $\epsilon(\mathbf{r}) = 1$ in the whole computational domain Ω . Note that atomic reaction field energies $\Delta G_{\text{RF}i}$ are used as features in our FFT based solvation model.

Here the reaction field energy gives a good description of the solvation free energy. In our earlier study on the solvation model, we found that reaction field energy related molecular descriptor provides a very accurate characterization of the solvation effects. The study of a large amount of small solute molecules demonstrates that by using these microscopic features in the solvation model, the predicted solvation free energy is in an excellent agreement with the experimental solvation free energy. For example, the RMSE of our leave-one-out test for a large database of 668 molecules is around 1 kcal/mol.⁸²

Note that in Eq. (9), the whole reaction field energy is regarded as the sum of atomic reaction field energies. In the PB calculation, the solute molecule is usually assumed to be a homogeneous dielectric continuum with a uniform dielectric constant, which is an inappropriate assumption, since atoms in different environments should have different dielectric properties.⁸⁶ For this reason, we select the atomic reaction field energy as a microscopic feature and let the machine learning algorithm to automatically take care the possible difference in dielectric constants.

Electrostatic binding features By using the PB model, we can further obtain the electrostatics contribution to the protein-ligand binding affinity. The electrostatics binding free energy is calculated by

$$\Delta G_{\text{el}} = (\Delta G_{\text{RF}})_{\text{Com}} - (\Delta G_{\text{RF}})_{\text{Pro}} - (\Delta G_{\text{RF}})_{\text{Lig}} + \Delta G_{\text{Coul}}, \quad (11)$$

where ΔG_{el} is the electrostatics binding free energy between protein and ligand, $(\Delta G_{\text{RF}})_{\text{Pro}}$ and $(\Delta G_{\text{RF}})_{\text{Lig}}$ are the reaction field energies of the protein and ligand, respectively. Here ΔG_{Coul} is the Coulombic interaction between the two parts in the vacuum environment, which is computed as

$$\Delta G_{\text{Coul}} = \sum_{i,j} \frac{Q_i Q_j}{r_{ij}}, \quad (12)$$

where r_{ij} is the distance between two specific charges, and indexes i and j run over all the atoms in the protein and ligand molecules, respectively. It is worthy to remind that the electrostatics binding free energy ΔG_{el} is a microscopic feature representing the contributions of solvation and Coulombic to the macroscopic binding free energy ΔG . The PB model is solved by our in-house software, MIBPB,^{15,27,91,98} which is shown to be grid size independent. Its relative ranking orders of reaction field energy and binding free energy calculated with different grid sizes are consistent.⁶¹ This numerical accuracy guarantees the preserving of relative ranking orders, which in turn avoids the influence on the prediction from numerical errors.

Atomic Coulombic interaction Coulombic energy plays an important role in the molecular mechanics energy.^{32,43,57} Coulombic energy calculation also depends on the dielectric medium. To this end, we considered the atomic Coulombic interactions in vacuum environment. Specifically, for the i th atom in the protein molecule, we select the microscopic feature from atomic Coulombic energy as

$$(\Delta G_{\text{Coul}})_i = \sum_j \frac{Q_i Q_j}{r_{ij}}, \quad (13)$$

where the summation index j runs over all the atoms in the ligand molecule. The Coulombic energy associated with the atoms in the ligand molecules can be defined analogously.

Atomic van der Waals interaction It was shown that van der Waals interactions play an important role in solvation analysis.^{17,19,24,80,83} We expect that van der Waals interactions are essential to binding process as well. In this work, we consider the 6-12 Lennard Jones (LJ) interaction potential for modeling the van der Waals interactions

$$u_{ij}(\mathbf{r}_i, \mathbf{r}_j) = \epsilon_{ij} \left[\left(\frac{r_i + r_j}{\|\mathbf{r}_i - \mathbf{r}_j\|} \right)^{12} - 2 \left(\frac{r_i + r_j}{\|\mathbf{r}_i - \mathbf{r}_j\|} \right)^6 \right], \quad (14)$$

where r_i and r_j are atomic radii of the i th and j th atoms, respectively. Here ϵ_{ij} measures the depth of the attractive well at $\|\mathbf{r}_i - \mathbf{r}_j\| = r_i + r_j$. For features related to the van der Waals interactions, we select pairwise particles interactions as microscopic features for describing the van der Waals interactions between the protein and ligand. In these features, each atom type is collected together, and well-depth parameters ϵ_{ij} are left as training parameters in the subsequent ranking procedure.

Atomic solvent excluded surface area and molecular volume Molecular surface area and surface enclosed volume are usually employed in scaled-particle theory (SPT) to model the nonpolar solvation free energy^{55,65,74} and/or entropy contribution to the protein ligand binding affinity. In our FFT-BP, the solvent excluded surface is employed for the conformation modeling of the solvated molecule. The molecular surface area associated with each atom type and molecular volume are used as microscopic features. These features are also computed by our in-house software, ESES,⁵² in which a second order convergent scheme based on the level set theory and third order volume schemes are implemented. In ESES, the molecular surface area is partitioned into atomic surface areas based on the power diagram theory.

Summary of microscopic features We consider microscopic features of a protein-ligand complex. For the protein molecule, microscopic features are selected from following types of atoms, namely, C, N, O, and S. For the ligand molecule, atomic features are collected from C, N, O, S, P, F, Cl, Br, and I. Here we drop features from hydrogen atoms (H) since the positions of these atoms are not typically given in original X-ray crystallography data, and their information may not be accurate. This selection of representative atoms is consistent with that of some other existing scoring functions, e.g., Cyscore,¹² AutoDock Vina,⁷⁶ and RF-Score.⁵ In our model, we collect electrostatic binding free energy, atomic reaction field energies, molecular reaction field energy, atomic van der Waals and Coulombic interactions, atomic surface areas, and molecular volume as the building block of feature space. Due to the fact that binding is a thermodynamic process, the change of the atomic reaction field energies, atomic surface areas, and molecular volumes between the bounded and unbounded states are selected as microscopic features as well.

For the atomic features associated with each type of element, we consider their corresponding statistical quantities, i.e., maximum, minimum and average, as features. Similarly, maximum, minimum and average of absolute values of atomic electrostatic features are also used features. All features used in the current work are summarized in Table 2.

Table 2: List of features and software used in protein-ligand binding energy prediction. Atom types X selected for protein are C, N, O and S. Atom types X selected for complex and ligand are C, N, O, S, P, F, Cl, Br and I. All structure inputs in each feature calculation are in PQR format. The procedure for acquiring this format is discussed in Section III.A.2

Features	Software
Reaction field Energies for complex/protein/ligand	MIBPB (http://weilab.math.msu.edu/MIBPB/)
Electrostatic binding free energies	MIBPB and Python
Molecular volumes for complex/protein/ligand	ESES (http://weilab.math.msu.edu/ESES/)
Molecular surface areas for complex/protein/ligand	ESES
Atomic van der Waals interactions between X atoms in protein and Y atoms in ligand	Python
Statistical quantities (sum,mean,max,min) of atomic reaction field energies for X atoms in complex/protein/ligand	MIBPB and Python
Statistical quantities (sum,mean,max,min) of atomic reaction field energies for X atoms in altogether complex, protein and ligand	MIBPB and Python
Statistical quantities (sum,mean,max,min) of atomic reaction field energies for all atoms in complex/protein/ligand	MIBPB and Python
Statistical quantities (sum,mean,max,min) of atomic reaction field energies for all atoms in altogether complex, protein and ligand	MIBPB and Python
Statistical quantities (sum,mean,max,min) of atomic surface areas for X atoms in complex/protein/ligand	ESES and Python
Statistical quantities (sum,mean,max,min) of atomic surface areas for X atoms in altogether complex, protein and ligand	ESES and Python
Statistical quantities (sum,mean,max,min) of atomic surface areas for all atoms in complex/protein/ligand	ESES and Python
Statistical quantities (sum,mean,max,min) of atomic surface areas for all atoms in altogether complex, protein and ligand	ESES and Python
Statistical quantities (sum,mean,max,min) of atomic Coulombic energies for X atoms in complex/protein/ligand	Python
Statistical quantities (sum,mean,max,min) of atomic Coulombic energies for X atoms in altogether complex, protein and ligand	Python
Statistical quantities (sum,mean,max,min) of atomic Coulombic energies for all atoms in complex/protein/ligand	Python
Statistical quantities (sum,mean,max,min) of atomic Coulombic energies for all atoms in altogether complex, protein and ligand	Python
Statistical quantities (sum,mean,max,min) of atomic charges for X atoms in complex	Python
Statistical quantities (sum,mean,max,min) of atomic charges for all atoms in complex	Python
Statistical quantities (sum,mean,max,min) of absolute values of atomic charges for X atoms in complex	Python
Statistical quantities (sum,mean,max,min) of absolute values of atomic charges for all atoms in complex	Python
Volume change between bounded and unbounded states	ESES and Python
Statistical quantities (sum,mean,max,min) of atomic reaction field energies change of X atoms in protein/ligand	MIBPB and Python
Statistical quantities (sum,mean,max,min) of atomic reaction field energies change of X atoms in both protein and ligand	MIBPB and Python
Statistical quantities (sum,mean,max,min) of atomic reaction field energies change of all atoms in protein/ligand	MIBPB and Python
Statistical quantities (sum,mean,max,min) of atomic reaction field energies change of all atoms in both protein and ligand	MIBPB and Python
Statistical quantities (sum,mean,max,min) of atomic area change of X atoms in protein/ligand	ESES and Python
Statistical quantities (sum,mean,max,min) of atomic area change of X atoms in both protein and ligand	ESES and Python

Table 2 – continued

Features	Software
Statistical quantities (sum,mean,max,min) of atomic area change of all atoms in protein/ligand	ESES and Python
Statistical quantities (sum,mean,max,min) of atomic area change of all atoms in both protein and ligand	ESES and Python

II.C Machine learning algorithm

Many machine learning algorithms, including support vector machine, decision tree learning, random forest, and deep neural network can be employed. A specific machine learning algorithms utilized in the present study to protein ligand binding affinity scoring is an MART algorithm. MART is a list-wise LTR algorithm, for a given training set with feature vectors and associated ranking order (here we simply using the protein-ligand binding affinity as this label value), it trains a function that optimally simulates the relation between features and labels. When applied to a protein-ligand complex in the test set, this trained function acts on the corresponding features and gives a predicted value. The predicted value reflects the binding affinity of the complex in the test set. In the web-search community, LambdaMART is one of the state-of-the-art LTR algorithms, here LambdaMART is a coupling of Lambda and MART. Compared to the classical MLR model for training functions that link features and labels, MART can capture the nonlinear relationship. Furthermore, compared to most neuron network based algorithms, it is more efficient. MART also named GBDT (gradient boosting decision tree) is a very efficient ensemble method for regression. Meanwhile, due to the boosting of the weaker learners (usually quite simple models like decision tree), the over-fitting problem can be avoided effectively. The principles of the GBDT are summarized as following:

- For the training set, GBDT successively learns the weak learners, and each weak learner is a regression tree with quite a few levels for fitting the residual of the previous forest compared to the training set. This procedure starts from a regression tree for fitting the training set, and the regression tree is added into the forest gradually. Each succeed regression tree is used for fitting the residual of the previous forest.
- Instead of counting the whole contribution from each regression tree, shrinkage is adopted, which is a weight of the regression tree. This weight is obtained through solving an optimization problem via the simple line searching algorithm.
- Weighted contributions from the whole regression trees are presented in the final scoring function, which is the boosting of simple regression trees. Due to the simplicity of each regression tree, the over-fitting problem can be bypassed efficiently.

In summary, the MART learns a function between features and the binding free energy through the training set. In the testing step, this function assigns a predicted binding affinity to each sample in the testing set, and the ranking position of a given sample is determined through the obtained score. This ranking method is significantly different from the classical pairwise approaches, e.g., RankSVM,^{37,38,45} where ranking is based on the pairwise comparison between all sample pairs in the training set. A major drawback of these approaches is that they assumes the same penalty for all pairs. In contrast, we only care about a few top ranking results for a given query in most applications. For more comprehensive and mathematical description of the MART, reader is referred to the literature.^{10,22} Many other LTR algorithms can be used in our framework as well, like LambdaMART,^{10,22} ListNet,¹³ etc.

II.D Method for binding affinity prediction

In this subsection, we discuss the FFT prediction of the binding free energy of a given target protein-ligand complex AB. Based on our assumption that binding free energy is a functional of feature vectors, we construct a feature function around the target molecular complex and use it to predict the binding free energy. Even though the exact form of the function between feature and binding affinity is unknown, locally it can be approximated by a linear function. In other words, locally we assume the binding affinity is a linear function of microscopic feature vectors.

The importance of various features can be ranked automatically during the machine learning procedure, and thus the number of influential features (n) can be reduced by selecting features of top importance to represent the binding affinity. We assume that target molecular complex AB is characterized by its feature vector $\mathbf{x}_{AB} = (\mathbf{x}_{AB1}, \mathbf{x}_{AB2}, \dots, \mathbf{x}_{ABn})$, where n is the dimension of the microscopic feature space, i.e., the space of all microscopic feature vectors. We also assume that by using the LTR algorithm, we can find top m nearest neighbors from the training set. The extended feature vectors of these nearest neighbor complexes are given by $\{\mathbf{v}_i = (\mathbf{x}_i, \Delta G_i)\}_{i=1}^m$. In general, the dimension of the feature space is much larger than the number of nearest neighbors used, i.e., $m \ll n$. Therefore, the direct least square approach may lead to over-fitting. To avoid over-fitting, we utilize a Tikhonov regularization based least square algorithm for training the binding

affinity function. From the extended feature vectors, we can set up the following set of equations

$$\begin{pmatrix} \Delta G_1 \\ \Delta G_2 \\ \vdots \\ \Delta G_m \end{pmatrix} = \begin{pmatrix} x_{11} & x_{12} & \cdots & x_{1n} \\ x_{21} & x_{22} & \cdots & x_{2n} \\ \vdots & \vdots & \vdots & \vdots \\ x_{m1} & x_{m2} & \cdots & x_{mn} \end{pmatrix} \begin{pmatrix} w_1 \\ w_2 \\ \vdots \\ w_n \end{pmatrix} + \begin{pmatrix} b \\ b \\ \vdots \\ b \end{pmatrix}, \quad (15)$$

where $w_i = w_i(\mathbf{v}_1, \mathbf{v}_2, \dots, \mathbf{v}_m)$ and $b = b(\mathbf{v}_1, \mathbf{v}_2, \dots, \mathbf{v}_m)$ define the function for ΔG_i . By the similarity assumption, the same functional form can be used for target complex AB. For further derivation, we rewrite Eq. (15) as

$$\Delta \mathbf{G} = \mathbf{x}\mathbf{w} + b\mathbf{1}, \quad (16)$$

where $\Delta \mathbf{G} = (\Delta G_1, \Delta G_2, \dots, \Delta G_m)^T$, $\mathbf{w} = (w_1, w_2, \dots, w_n)^T$, $\mathbf{1}$ is an m -dimensional column vector with all elements equaling 1, and matrix \mathbf{x} is given by

$$\mathbf{x} = \begin{pmatrix} x_{11} & x_{12} & \cdots & x_{1n} \\ x_{21} & x_{22} & \cdots & x_{2n} \\ \vdots & \vdots & \vdots & \vdots \\ x_{m1} & x_{m2} & \cdots & x_{mn} \end{pmatrix}.$$

To avoid over-fitting, we add an L_2 penalty to the weight vector \mathbf{w} , and solve Eq. (16) as an optimization problem

$$\min_{\mathbf{w}, b} \|\Delta \mathbf{G} - \mathbf{x}\mathbf{w} - b\mathbf{1}\|_2^2 + \lambda \|\mathbf{w}\|_2^2 := \min_{\mathbf{w}, b} \mathbf{F}, \quad (17)$$

where λ is a regularization parameter and is set to 10 in this work, and $\|\cdot\|_2$ denotes the L_2 norm of the quantity $*$.

By solving $\frac{\partial \mathbf{F}}{\partial \mathbf{w}} = 0$, we have

$$\mathbf{w} = (\mathbf{x}^T \mathbf{x} + \lambda \mathbf{I})^{-1} (\mathbf{x}^T \Delta \mathbf{G} - \mathbf{x}^T (b\mathbf{1})), \quad (18)$$

where \mathbf{I} is an $m \times m$ identity matrix.

To determine b from Eq. (17), we relax $b\mathbf{1}$ to an arbitrary vector such that $\mathbf{b} = (b_1, b_2, \dots, b_m)^T$. By solving $\frac{\partial \mathbf{F}}{\partial \mathbf{b}} = 0$, we have

$$\mathbf{b} = \Delta \mathbf{G} - \mathbf{x}\mathbf{w}. \quad (19)$$

An unbiased estimation of b is given by

$$b = \frac{\sum_{i=1}^m (\Delta \mathbf{G} - \mathbf{x}\mathbf{w})_i}{m}, \quad (20)$$

where $(\Delta \mathbf{G} - \mathbf{x}\mathbf{w})_i$ is the i th component of the vector $\Delta \mathbf{G} - \mathbf{x}\mathbf{w}$.

The optimization problem in Eq. (17) is solved by alternately iterating Eqs. (18) and (20), which is essentially an expectation - maximization (EM) algorithm.

After obtaining optimized weights \mathbf{w} for the feature vector \mathbf{x} and hyperplane height b , the binding free energy of target molecular complex AB can be predicted as

$$\Delta G_{AB} = b + \sum_{i=1}^n w_i \mathbf{x}_{ABi}. \quad (21)$$

Equation (21) can be regarded as a linear approximation of the binding free energy functional $\Delta G_{AB} = f(\mathbf{x}_{AB}, \mathbf{v}_1, \mathbf{v}_2, \dots, \mathbf{v}_m)$.

Alternatively, we can also directly obtain the binding affinity of the target complex AB from the LTR ranking value if the ranking algorithm attempts to fit the target value. For general LTR algorithms, especially pairwise ranking algorithms, the direct use of the ranking score as a predicted binding affinity is not appropriate. However, the proposed protocol also applies to this scenario. These two approaches are compared in this present work.

III Numerical results

In this section, we explore the validity, demonstrate the performance, and examine the limitation of the proposed FFT-BP. First, we describe datasets used in this work. Then, we examine whether FFT-BP's performance depends on protein clusters, where each cluster contains one specific protein and tens or hundreds of ligands. Our test on a validation set of 1322 protein-ligand complexes from 7 clusters indicates that the performance of the proposed FFT-BP does not depend on protein clusters. By using the same test set, we also study the impact of cut-off distance to FFT-BP prediction. Here cut-off distance refers to a protein feature evaluation truncation distance. Protein atoms within the cut-off distance are allowed to contribute the atomic feature selection and calculation (except for molecule-wise features, such as volume, electrostatic solvation free energy, electrostatic binding free energy, etc). To further benchmark the accuracy of the present FFT-BP, we carry out a five-fold cross validation on training set ($N = 3589$), which is derived from the PDBBind v2015 refined set.⁵⁴ Finally, we provide blind predictions on a benchmark set of 100 protein-ligand complexes,⁸⁶ the PDBBind v2007 core set ($N = 195$),⁵ and the PDBBind v2015 core set ($N = 195$).⁵⁴

III.A Dataset preparation

All data sets used in the present work are obtained from the PDBBind database,⁵⁴ in which the PDBBind v2015 refined set of 3,706 entries was selected from a general set of 14,620 protein-ligand complexes with good quality, filtered over binding data, crystal structures, as well as the nature of the complexes.⁵⁴ Due to the feature extraction, a pre-processing of data is required in the present method.

III.A.1 Datasets

This work utilizes one validation set ($N = 1322$), one training set ($N = 3589$), and three test sets ($N = 195$, $N = 195$ and $N = 100$) as described below.

Validation set ($N = 1322$) To explore the cluster dependence (or independence) and the optimal cut-off distance of the present FFT-BP, we select a subset of the PDBBind v2015 refined set with 1322 complexes in 7 different clusters. Each cluster contains one protein and a large number, ranging from 93 to 333, of small ligand molecules. With this validation, we examine whether the predictions inside various clusters are more accurate than the overall prediction regardless of clusters. The performance dependence of the cut-off distance is also explored with this set.

Training sets For the PDBBind v2015 refined set, we carry our FFT microscopic feature extraction via appropriate force field parametrization described below, which leads to a parametrized set of 3589 protein-ligand complexes. The training set is employed to train our FFT model according to each test. Whenever a test set is studied, its entries are carefully excluded from the training set of 3589 complexes and then, the model is trained without any test set molecule. Similarly, we apply our FFT approach for training another training set, namely PDBBind v2007 refined set, comprising 1082 complexes.

Test sets Three test sets are standard ones described in the literature. PDB IDs of the training set and the validation set are given in the Supporting material.

The PDBBind v2015 core set of 195 benchmark-quality complexes is employed as a test set. According to the literature,⁵⁴ the PDBBind v2015 core set was selected with an emphasis on the diversity in structures and binding data. It contains 65 representative clusters from the PDBBind v2015 refined set. For each cluster, it must have at least five protein-ligand complexes and three complexes, one with the highest binding constant, another with the lowest binding constant, and the other with a medium binding constant were selected for the PDBBind v2015 core set.⁵⁴

We also consider two additional test sets, *the PDBBind v2007 core set* of 195 complexes¹⁸ and *the benchmark set* of 100 complexes⁸⁶ to benchmark the proposed FFT-BP against a large number of scoring functions.

III.A.2 Data pre-processing

FFT-BP utilizes microscopic features, which requires appropriate feature extraction from the data set. Before the feature generation, structure optimization and force field assignment are carried out. Protein structures with corresponding ligand are prepared with the protein preparation wizard utility of the Schrödinger 2015-2 Suite^{23,70} with default parameters except filling the missing side chains. The protonation states for ligands are generated using Epik state penalties and the H-bond networks for the complex are further optimized using PROPKA at pH 7.0.^{63,69} The restrained minimization on heavy atoms for the complex structures are finally performed with OPLS 2005 force field.⁴¹ The atomic radii and charges for the complexes are parametrized by Amber tool14.¹⁴ For ligand molecules, charges are calculated by the antechamber module with AM1-BCC semi-empirical charge method and the atomic radii are assigned by using the mbondi2 radii set.³⁶ For protein molecules, radii and charges of each atom are parametrized by the Amber ff14SB general force field with tleap module.¹⁴

Protein features are extracted with a cut-off distance. Specifically, we first find a tight bounding box containing the ligand, then extend feature generation domain along all directions around the box to a cut-off distance. We provide all the data involved in this work in the Supporting material, in which some protein-ligand structures that need specific treatments are highlighted.

In the PDBBind database, the protein ligand binding affinity is provided in term of pK_d . We convert all the energy unit in the PDBBind database to kcal/mol. To derive the unit convert formula, one notes that

$$\Delta G = RT \ln k_d = -RT \ln K_{eq},$$

where ΔG is the Gibbs free energy, k_d is the disassociation constant, and R is the gas constant. Since $pK_d = -\log_{10} K_d$, then at the room temperature, $T = 298.15K$, one has the following relation between these two units

$$\Delta G = -1.3633 pK_d. \quad (22)$$

III.B Validation

In this section, we explore the properties of FFT-BP and validate its performance. The following two important issues are examined in several existing scoring functions. The first issue is related to the protein-ligand binding affinity prediction of diverse multiple clusters, especially clusters with limited experimental data. Another issue is that a scoring method should be optimized with a cut-off distance in the feature extraction to maintain sufficient accuracy and avoid unnecessary feature calculations. In the existing work, the LTR based scoring functions can predict cross-cluster binding affinity well.⁹³ For the random forest and some other machine learning algorithms, one typically selects a cut-off distance of 12 Å, in the protein feature calculation.⁶

In this work, we demonstrate the capability of the FFT-BP for the accurate cross-cluster binding affinity prediction. Additionally, we explore the optimal cut-off distance for FFT-BP feature extraction. Finally, since the accuracy of the FFT-BP

Table 3: The RMSEs (kcal/mol) for the five-fold validation on the 7 clusters of the validation set and on the whole validation set ($N = 1322$) with 10 different cut-off distances in the feature extraction.

Test set	Group	Cut-off distance									
		5 Å	10 Å	15 Å	20 Å	25 Å	30 Å	35 Å	40 Å	45 Å	50 Å
Cluster 1	Group1	1.90	1.86	1.76	1.73	1.81	1.90	1.81	1.82	1.82	1.86
	Group2	2.07	2.15	2.38	2.23	2.35	2.25	2.21	2.24	2.24	2.24
	Group3	2.31	1.98	2.04	1.95	1.85	1.87	1.87	1.89	1.90	1.90
	Group4	1.89	1.75	1.58	1.63	1.63	1.67	1.62	1.66	1.65	1.65
	Group5	2.35	2.22	2.09	2.05	2.14	1.67	2.10	2.12	2.12	2.13
	Average	2.11	2.01	1.99	1.93	1.97	2.13	1.93	1.96	1.96	1.97
Cluster 2	Group1	1.39	1.33	1.31	1.32	1.39	1.43	1.46	1.42	1.42	1.44
	Group2	1.66	1.24	1.31	1.23	1.19	1.14	1.15	1.19	1.19	1.19
	Group3	1.39	1.28	1.14	1.21	1.28	1.31	1.37	1.37	1.32	1.32
	Group4	1.44	1.33	1.35	1.36	1.37	1.38	1.35	1.40	1.30	1.40
	Group5	1.53	1.44	1.38	1.49	1.36	1.37	1.38	1.33	1.38	1.29
	Average	1.49	1.33	1.34	1.32	1.32	1.33	1.34	1.35	1.33	1.33
Cluster 3	Group1	2.56	2.40	2.65	2.41	2.53	2.62	2.61	2.60	2.60	2.60
	Group2	2.07	2.13	2.08	2.10	2.11	2.11	2.11	2.09	2.09	2.09
	Group3	1.54	1.53	1.52	1.57	1.55	1.51	1.52	1.50	1.50	1.50
	Group4	1.82	1.75	1.70	1.71	1.64	1.68	1.70	1.72	1.72	1.72
	Group5	2.14	2.23	2.20	2.15	2.18	2.26	2.26	2.27	2.27	2.27
	Average	2.05	2.03	2.07	2.01	2.03	2.08	2.08	2.08	2.08	2.08
Cluster 4	Group1	1.59	1.78	1.80	1.88	1.76	1.68	1.72	1.72	1.76	1.81
	Group2	1.41	1.47	1.53	1.25	1.34	1.39	1.37	1.34	1.37	1.37
	Group3	1.58	1.46	1.50	1.59	1.56	1.52	1.55	1.55	1.53	1.55
	Group4	1.91	1.76	1.76	1.87	1.83	1.84	1.80	1.78	1.81	1.87
	Group5	1.57	1.54	1.61	1.73	1.81	1.84	1.74	1.67	1.75	1.74
	Average	1.62	1.61	1.64	1.68	1.67	1.67	1.65	1.62	1.65	1.68
Cluster 5	Group1	2.01	2.43	1.83	1.64	1.60	1.65	1.67	1.69	1.65	1.67
	Group2	2.15	2.08	1.89	1.88	1.92	1.86	1.94	1.88	1.92	1.87
	Group3	2.52	2.26	2.54	2.42	2.41	2.37	2.39	2.40	2.35	2.35
	Group4	1.65	1.70	1.30	1.37	1.25	1.33	1.35	1.36	1.34	1.30
	Group5	3.18	2.87	2.89	2.49	2.59	2.54	2.56	2.67	2.65	2.65
	Average	2.39	2.31	2.18	2.03	2.03	2.02	2.05	2.07	2.06	2.05
Cluster 6	Group1	3.17	2.99	3.03	2.95	3.00	3.02	2.90	2.92	2.92	2.92
	Group2	2.09	1.83	1.83	1.82	1.91	1.83	1.88	1.86	1.86	1.86
	Group3	1.68	1.71	1.55	1.65	1.69	1.55	1.63	1.58	1.56	1.56
	Group4	1.73	1.69	1.55	1.60	1.60	1.51	1.58	1.58	1.59	1.59
	Group5	2.30	1.97	2.04	2.13	2.03	2.06	2.05	2.05	2.05	2.05
	Average	2.26	2.09	2.08	2.09	2.10	2.07	2.06	2.06	2.06	2.06
Cluster 7	Group1	1.83	1.97	2.16	1.93	1.68	1.66	2.01	1.90	1.88	1.91
	Group2	1.92	1.99	1.97	1.97	2.00	1.93	2.09	2.06	2.28	2.21
	Group3	1.68	1.69	1.45	1.39	1.35	1.39	1.44	1.51	1.54	1.45
	Group4	2.27	2.11	2.13	1.91	2.14	2.14	2.39	2.36	2.27	2.42
	Group5	1.76	1.40	1.29	1.32	1.41	1.35	1.38	1.39	1.44	1.45
	Average	1.90	1.83	1.81	1.71	1.73	1.71	1.88	1.86	1.90	1.91
Average over all 7 clusters		1.90	1.88	1.87	1.83	1.84	1.84	1.85	1.85	1.85	1.86
Whole set	Group1	1.81	1.55	1.62	1.57	1.67	1.69	1.66	1.55	1.52	1.57
	Group2	1.63	1.76	1.62	1.69	1.64	1.67	1.55	1.71	1.73	1.69
	Group3	1.71	1.58	1.65	1.65	1.65	1.55	1.55	1.63	1.51	1.66
	Group4	1.73	1.62	1.65	1.57	1.56	1.53	1.78	1.57	1.69	1.59
	Group5	1.64	1.65	1.59	1.64	1.65	1.68	1.60	1.63	1.67	1.64
	Average	1.70	1.63	1.63	1.63	1.64	1.63	1.64	1.63	1.64	1.64

predictions depends on the numbers of the nearest neighbors and top features, we investigate robustness of the proposed FFT-BP with respect to choices of the nearest neighbors and top features.

Two sets of protein-ligand complexes, i.e., the validation set ($N = 1322$) and the training set ($N = 3589$), are employed in this validation study.

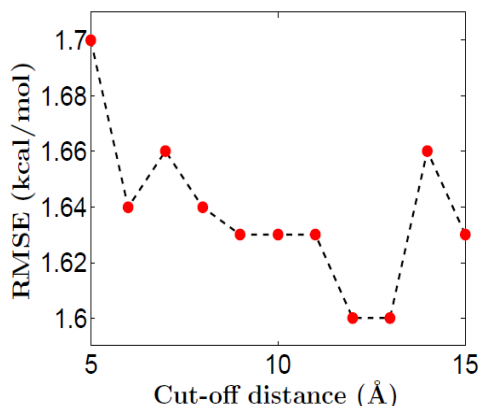


Figure 1: The prediction RMSE vs the cut-off distance for the validation set ($N = 1322$).

Table 4: The RMSEs (kcal/mol) for the five-fold test on the validation set ($N = 1322$) with FFT-BP calculated at different cut off distances.

Group	Cut-off distance										
	5 Å	6 Å	7 Å	8 Å	9 Å	10 Å	11 Å	12 Å	13 Å	14 Å	15 Å
Group1	1.81	1.68	1.80	1.58	1.61	1.55	1.49	1.62	1.50	1.60	1.62
Group2	1.63	1.67	1.61	1.79	1.67	1.76	1.63	1.65	1.76	1.72	1.62
Group3	1.71	1.68	1.57	1.65	1.61	1.58	1.80	1.62	1.56	1.71	1.65
Group4	1.73	1.56	1.46	1.58	1.64	1.62	1.74	1.58	1.55	1.70	1.65
Group5	1.64	1.57	1.82	1.57	1.60	1.65	1.46	1.56	1.59	1.59	1.59
Average	1.70	1.64	1.66	1.64	1.63	1.63	1.63	1.60	1.60	1.66	1.63

III.B.1 Validation on the validation set ($N = 1322$)

We validate the proposed FFT-BP on the validation set of 1322 complexes. We utilize the five-fold cross validation strategy to test the model and determine optimal cut-off distance. In this strategy, the validation set of 1322 complexes is randomly partitioned into five essentially equal sized subsets. Of the five subsets, a single subset is retained as the test set for testing the FFT-BP, and the remaining four subsets are used as training data. First, we run a coarse test with cut-off distance from 5 to 50 Å using 5 Å as the step size, which helps to determine a rough optimal cut-off distance. Second, we carry a refined search for the optimal the cut-off distance based on coarse test results with a step of size 1 Å. At a given cut-off size, we do the five-fold cross validation on the validation set of 1322 complexes, together with the five-fold cross validation on each of 7 clusters. Table 3 lists the RMSEs on all the five-fold cross validation with cut-off distance 5 to 50 Å and step size 5 Å.

Results in Table 3 indicate that: 1) Overall, prediction over the whole set of 1322 complexes gives better results than predictions on individual clusters. Therefore, the proposed method favors blind cross-cluster predictions. 2) According to the results from the whole validation set tests, feature cut-off distance at 10 Å has reached an optimal value. This distance is actually consistent with the explicit solvent modeling in which a 10 Å cut-off distance is designed to account for long range electrostatic interactions. To better estimate the optimal cut-off distance, we carry out a more accurate searching in the range of 5 to 15 Å distance with a step size of 1 Å. Table 4 lists the RMSEs of the five-fold cross validation on the whole validation set of 1322 complexes. These results show that 12 Å is the optimal cut-off distance in the searched solution space, which is consistent with that used in the RF-Score.⁶ We plot the relation between the cut-off distance and prediction error in Fig. 1. In the rest of this work, the cut-off distance of 12 Å is utilized.

Finally, all the above predictions are based on the LTR ranking results. Alternatively, we can also carry out the prediction by using nearest neighbors and their associated features. We are interested to see the difference between these two approaches. To this end, we compute the binding affinities of five-fold results with different numbers of nearest neighbors and top features. Here top features are ranked by the LTR algorithm automatically according to their importance during the complex ranking. We list the top 50 important features to the protein ligand binding for the validation set in the Supporting material. We noted that the most important five features are the volume change, atomic Coulombic interaction of S atoms, area change of the C atoms in the protein and complex parts, and electrostatic binding free energy.

The RMSEs of the tests with different numbers of top features and nearest neighbors involved are presented in Table 5. The optimal result is obtained when four nearest neighbor and 10 top features are utilized, with RMSE 1.57 kcal/mol. It is seen that when less than or equal to 10 top features are employed the prediction is quite accurate. However, with more features and more neighbors involved, the prediction become slightly worse. One possible reason is that the quality of the nearest neighbors is reduced when more neighbors are involved in the prediction. Indeed, the neighbors that are not very close to the target molecule complex may make a large difference to the prediction accuracy of the target complex. This issue also motivates us to seek a better set of features for protein-ligand binding analysis.

Figure 2 depicts the optimal prediction results (Left chart) and RMSEs for each group (Right chart). It is seen that the RMSEs for all groups are almost the same, indicating the unbiased nature of five-fold cross-validation. The success of proposed FFT-BP is implied by the small RMSEs of 1.55 ~ 1.59 kcal/mol and the high overall Pearson correlation of 0.80.

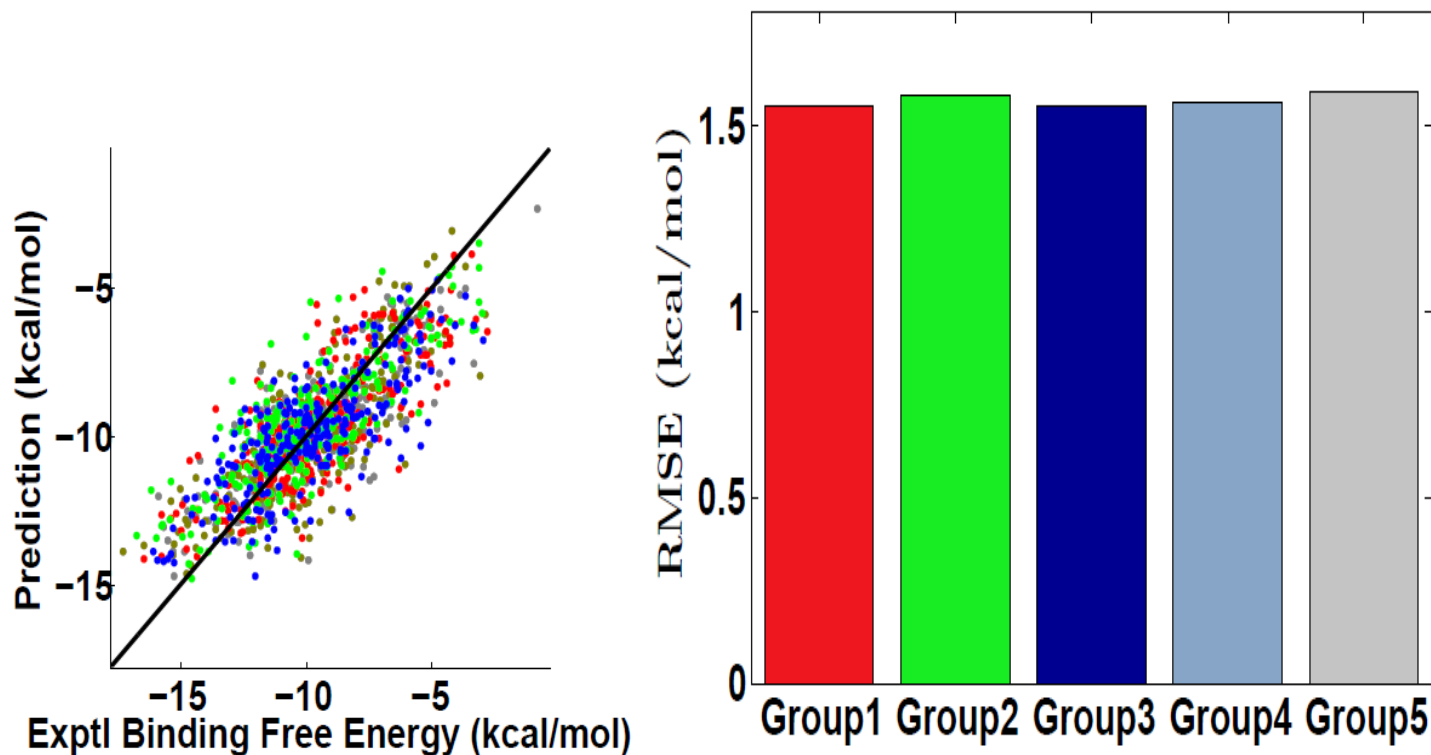


Figure 2: Five-fold cross validation on the validation set ($N = 1322$). Left chart: correlation between experimental binding affinities and FFT-BP predictions. Right chart: RMSEs for five groups. Here, RMSEs are 1.55, 1.58, 1.55, 1.56, and 1.59 kcal/mol for five groups, respectively. Overall Pearson correlation to the experimental binding affinities is 0.80.

Table 5: The RMSEs (kcal/mol) for the validation set ($N = 1322$) with different numbers of nearest neighbors and top features.

Number of nearest neighbors	Number of top features									
	5	10	15	20	25	30	35	40	45	50
1	1.60	1.60	1.60	1.61	1.61	1.61	1.61	1.61	1.61	1.62
2	1.60	1.60	1.61	1.61	1.61	1.61	1.61	1.62	1.62	1.62
3	1.60	1.59	1.60	1.70	1.66	1.68	1.71	1.70	1.69	1.70
4	1.61	1.57	1.62	1.71	1.70	1.72	1.73	1.70	1.85	1.83
5	1.61	1.60	1.67	1.74	1.75	1.74	1.75	1.73	1.78	1.77
6	1.62	1.61	1.68	1.79	1.80	1.81	1.81	1.88	1.85	1.85
7	1.61	1.61	1.65	1.78	1.77	1.78	1.78	1.81	1.82	1.82
8	1.62	1.62	1.65	1.74	1.76	1.76	1.77	1.78	1.80	1.81
9	1.62	1.61	1.65	1.74	1.75	1.76	1.76	1.76	1.78	1.77
10	1.62	1.62	1.73	1.74	1.79	1.80	1.82	1.82	1.88	1.90

III.B.2 Validation on the training set ($N = 3589$)

We also consider the five-fold cross validation on our training set of 3589 complexes. We randomly divide this data set into five groups with 717, 718, 718, 718, and 718 complexes, respectively. In the five-fold cross validation, each time we regard one group of molecules as the test set without binding affinity data, and using the remaining four groups to predict the binding affinities of the selected test set.

Directly using the ranking score as the predicted binding affinity leads to RMSE 2.00 kcal/mol. Alternatively, we can predict binding affinities using the nearest neighbors and top features.

Table 6 shows the RMSEs for the five-fold cross validation test on the training set ($N = 3589$). The number of nearest neighbors is varied from 1 to 10 and the number of top features is changed from 5 to 50. The most important 50 features indicated from the LTR algorithm are provided in the Supporting material. Five top important features are volume change, electrostatics binding free energy, and van der Waals interactions between C-S, C-O and C-N pairs, respectively. The optimal prediction is achieved when 8 nearest neighbors and top 15 features are used for binding affinity prediction, with the RMSE being 1.98 kcal/mol. Different numbers of nearest neighbors and top features basically give very consistent predictions. Compared to the five-fold test on the 1322 protein ligand complexes, the prediction errors on this set are much larger, which is partially due to the fact that structures in this test set is more complexes. For example, binding-site metal effects are presented without an appropriate treatment. We believe a better treatment of metal effects and a classification of ligand molecules would improve the FFT-BP prediction.

Table 6: The RMSEs (kcal/mol) for the five-fold cross validation on the training set ($N = 3589$) with different number of nearest neighbors and top features.

Number of nearest neighbors	Number of top features									
	5	10	15	20	25	30	35	40	45	50
1	2.00	1.99	2.00	2.00	2.00	2.01	2.01	2.01	2.01	2.02
2	2.00	1.99	2.00	1.99	2.00	2.01	2.01	2.01	2.01	2.01
3	2.01	2.00	2.00	2.00	2.00	2.00	2.02	2.01	2.01	2.01
4	2.00	2.01	2.00	1.99	2.00	2.01	2.01	2.01	2.02	2.01
5	2.01	2.00	2.01	2.01	2.01	2.01	2.01	2.01	2.01	2.02
6	2.00	1.99	1.99	2.00	2.00	2.01	2.01	2.01	2.01	2.01
7	2.00	2.00	2.00	2.00	2.01	2.01	2.02	2.02	2.02	2.02
8	2.00	1.99	1.98	1.99	1.99	2.00	2.00	2.00	2.01	2.00
9	2.00	2.00	2.00	2.01	2.02	2.05	2.05	2.05	2.05	2.04
10	1.99	2.00	2.00	2.03	2.04	2.07	2.08	2.08	2.08	2.08

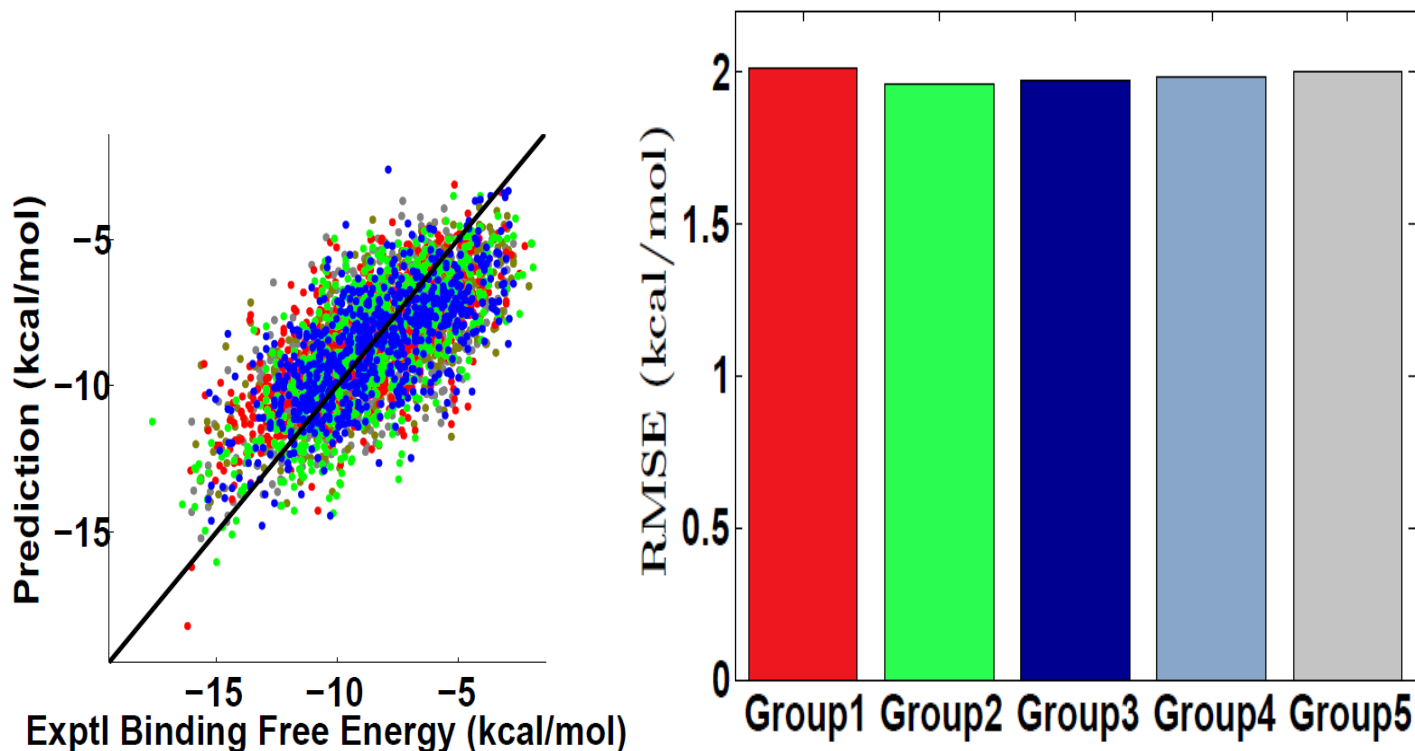


Figure 3: Five-fold cross validation on the training set (3589 complexes). Left chart: correlation between experimental binding affinities and FFT-BP predictions. Right chart: RMSEs for five groups. Here, RMSEs are 2.01, 1.96, 1.97, 1.98, and 2.00 kcal/mol for five groups, respectively. Overall Pearson correlation to the experimental is 0.70.

Figure 3 depicts the optimal prediction results (Left chart) and RMSEs for each group (Right chart). These tests demonstrate the following two facts. First, five-fold cross validation prediction is unbiased. The prediction results do not depend on the data itself and the RMSEs for all groups are almost at the same level. Second, when the protein-ligand complexes become diverse, the prediction becomes slightly worse due to the lack of similar complexes for certain clusters.

III.C Blind predictions on three test sets

To further verify the accuracy of the FFT-BP, we perform the blind prediction on three benchmark test sets. The training set ($N = 3589$) that is processed from the PDBBind v2015 refined set is utilized for the training in blind predictions of the benchmark set of 100 complexes and PDBBind v2015 core set. In addition, the training set ($N = 1082$) processed from PDBBind v2007 refined set is employed as the training data in a blind prediction of PDBBind v2007 core set. Due to the LTR algorithm used in our FFT-BP, the RMSE and correlation of our FFT-BP prediction would be around 0 kcal/mol and 1, respectively, had we include all the test set complexes in our training set. Therefore, in each blind prediction, we carefully exclude the overlapping test set complexes from the training set and re-train the training set with a reduced number of complexes.

III.C.1 Prediction on the benchmark set ($N = 100$)

First of all, we consider a popular benchmark set originally used by Wang *et al.*⁸⁶ This set contains 100 protein ligand complexes which involves a large variety of protein receptors. Originally this test set was used to test the performance of a large amount of well-known scoring functions and docking algorithms.⁸⁶ Recently, Zheng *et al.* have utilized this test set to

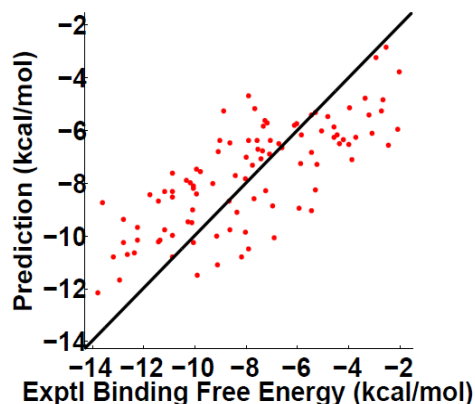


Figure 4: The correlation between experimental binding free energies and FFT-BP predictions on the benchmark test set ($N = 100$) with the RMSE of 1.99 kcal/mol and the Pearson correlation of 0.75.

Table 7: The RMSEs (kcal/mol) of the FFT-BP for the benchmark test set ($N = 100$) with different numbers of nearest neighbors and top features.

Number of nearest neighbors	Number of top features									
	5	10	15	20	25	30	35	40	45	50
1	2.00	2.00	2.00	2.00	2.00	2.00	2.00	2.00	2.00	2.00
2	2.01	2.01	1.99	1.99	2.01	2.00	2.01	2.01	2.01	2.01
3	2.00	2.00	2.00	2.00	2.00	2.00	2.00	2.01	2.01	2.01
4	2.01	2.01	2.01	2.00	2.00	2.00	2.01	2.01	2.01	2.01
5	2.01	2.01	2.01	2.01	2.01	2.01	2.00	2.01	2.01	2.01
6	2.02	2.01	2.01	2.01	2.01	2.01	2.01	2.01	2.01	2.01
7	2.02	2.02	2.01	2.01	2.01	2.01	2.01	2.01	2.01	2.01
8	2.01	2.01	2.01	2.01	2.01	2.01	2.02	2.02	2.02	2.02
9	2.01	2.01	2.01	2.01	2.01	2.01	2.02	2.01	2.01	2.01
10	2.01	2.01	2.01	2.02	2.01	2.02	2.01	2.02	2.02	2.02

demonstrate the superb performance of their KECSA method.⁹⁵ In this work, we examine the accuracy and robustness of our FFT-BP on this benchmark test set.

Directly using the ranking score as the predicted binding affinity leads to the RMSE of 2.01 kcal/mol and Pearson correlation coefficient of 0.75. Alternatively, we examine FFT-BP predictions using different numbers of nearest neighbors and top features. Table 7 lists the predicted RMSEs for the benchmark set ($N = 100$). The numbers of nearest neighbors and top features vary from 1 to 10 and from 5 to 50, respectively. The most important 50 features indicated by the LTR algorithm are provided in the Supporting material. Five top important features are volume change, electrostatics binding free energy, van der Waals interaction between C-S and C-C pairs, and the complex's area change. The optimal prediction is reached when 2 nearest neighbors and top 15 or 20 features are used for binding prediction. The corresponding RMSEs and correlation coefficients for both cases are 1.99 kcal/mol and 0.75, respectively. Different numbers of nearest neighbors and top features basically give rise to very consistent predictions. We also note that the prediction errors for this 100 test set are very similar to those of the five-fold cross validation tests on our training set ($N = 3589$). This consistency indicates the robustness of the proposed FFT-BP in binding affinity predictions.

Figure 4 illustrates the optimal prediction results compared to the experimental data. The RMSE and Pearson correlation coefficient are 1.99 kcal/mol and 0.75, respectively. This test set is a critical test set with diverse protein-ligand complexes and a wide range of experimental binding free energies. In our prediction, most predictions are quite appealing with less than 2 kcal/mol RMSE compared to experimental results.

Many outstanding scoring functions have been tested on this test set as summarized by Zheng *et al.*⁹⁵ Here we also add our prediction to this list. As shown in Fig. 5, the performance of our FFT-BP is highlighted with red color. The performance of other 19 scoring functions are due to the courtesy of Ref.⁹⁵

III.C.2 Prediction on the PDBBind v2007 core set ($N = 195$)

PDBBind v2007 core set ($N = 195$) which contains high quality data mainly aims for testing the performance of scoring functions.⁵⁴ It has been employed to study and compare many excellent scoring functions.^{4,5,18,47,48} To predict the binding affinity of this core set, it is a rational to employ the PDBBind v2007 refined set instead of v2015 one as the training set. Definitely, the training set here will not overlap with the test set. The score from the MART machine learning method is directly used for the prediction. Figure 6 illustrates the correlation between experimental binding free energies and the best predictions obtained by the FFT-BP. The Pearson correlation coefficient and RMSE by FFT-BP are, respectively, 0.80 and 2.03 kcal/mol.

Li *et al* have given a comparison of tests on the PDBBind v2007 core set ($N = 195$) using many outstanding scoring functions.⁴⁸ In this regarding, we also plot the performance of our FFT-BP in terms of Pearson correlation coefficient in Fig. 7. The FFT-BP correlation coefficient of 0.80 is highlighted with red color.

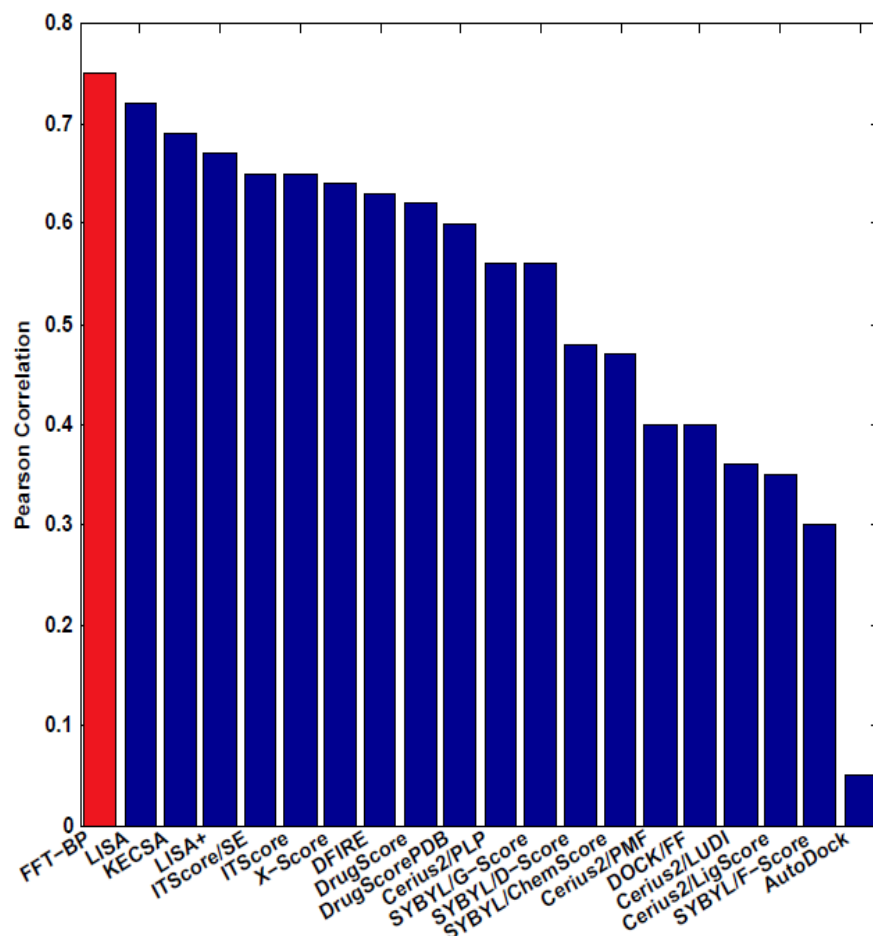


Figure 5: Performance comparison between different scoring functions on the benchmark test set ($N = 100$). The binding affinity comparisons was done for FFT-BP, and 19 well-known scoring functions, namely LISA, KECSA, LISA+,^{94,95} ITScore/SE,³⁵ ITScore,³⁴ X-Score,⁸⁵ DFIRE,⁹² DrugScoreCSD,⁷⁷ DrugScorePDB,³⁰ Cerius2/PLP,²⁶ SYBYL/G-Score,³⁹ SYBYL/D-Score,⁵⁸ SYBYL/ChemScore,²¹ Cerius2/PMF,⁶⁰ DOCK/FF,⁵⁸ Cerius2/LUDI,⁹ Cerius2/LigScore,¹ SYBYL/F-Score,⁶⁷ and AutoDock.⁵⁹

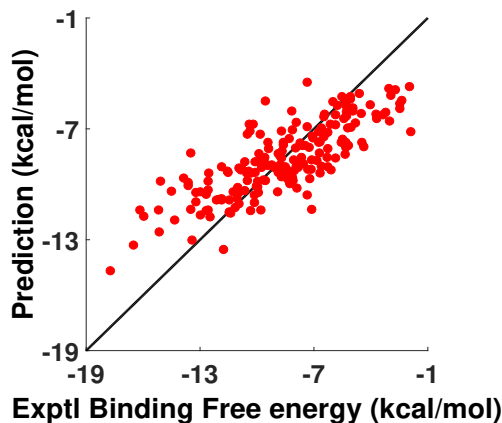


Figure 6: The correlation of between experimental binding free energies and FFT-BP predictions on the PDBBind core 2007 ($N = 195$). The RMSE and Pearson correlation coefficient are 2.02 kcal/mol and 0.80, respectively.

III.C.3 Prediction on the PDBBind v2015 core set ($N = 195$)

Finally, we perform a test on the PDBBind v2015 core set ($N = 195$), which contains high quality experimental data. PDBBind v2015 core set is the same as PDBBind v2013 core set and PDBBind v2014 core set. This test set is also quite challenging due its diversity of 65 protein-ligand clusters and a wide binding affinity range. In a similar routine, we first consider the FFT-BP prediction with different numbers of neighbors and top features. Table 8 shows the RMSEs of FFT-BP for PDBBind v2015 core set ($N = 195$). The top 50 features are also listed in the Supporting material. The most important features are similar to those in previous tests, which indicates that the volume change, electrostatic binding free energy and van der Waals interactions are of fundamental importance to the protein-ligand binding. It is worth noting that the RMSEs of FFT-BP predictions are lower than those from earlier test sets. A possible reason is that this data set is consistent with the training set as both obtained from the PDBBind 2015 refined set. Additionally, a better data quality might also contribute our better predictions. Our optimal prediction has the RMSE of 1.92 kcal/mol and Pearson correlation coefficient of 0.78, when

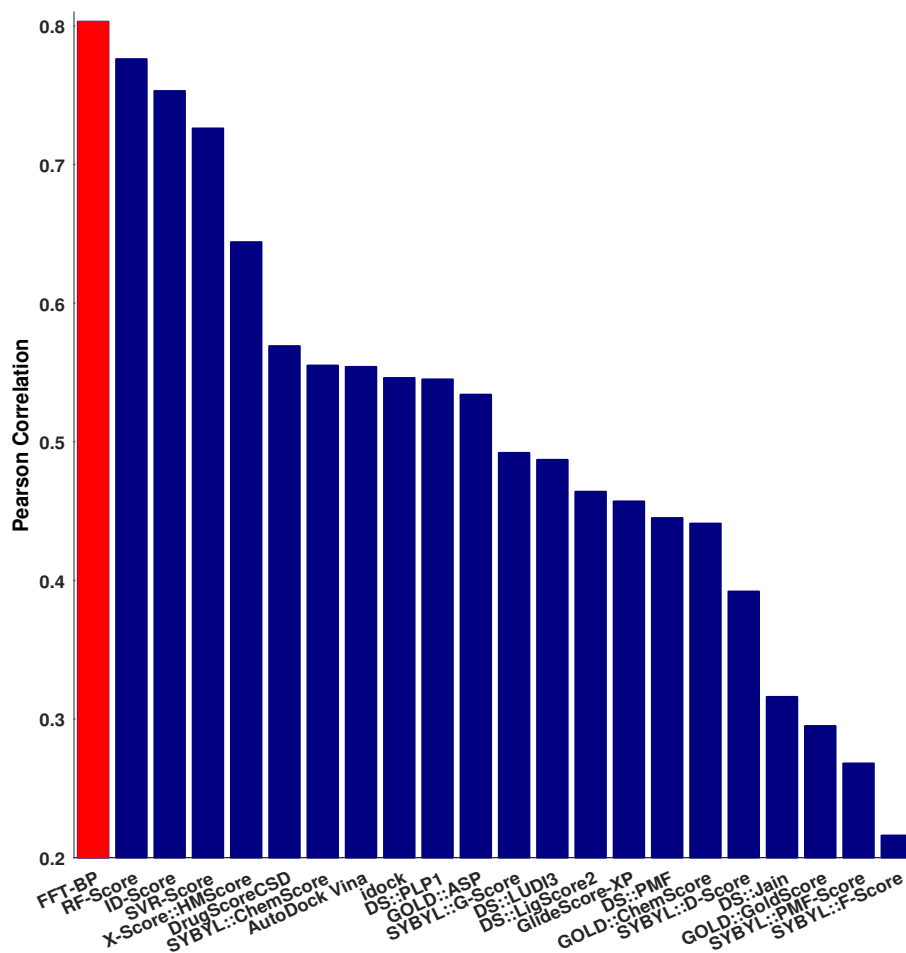


Figure 7: Performance comparison between different scoring functions on the PDBBind v2007 core set ($N = 195$). The performances of the other scoring function are adopted from the literature.^{4,5,18,47,48}

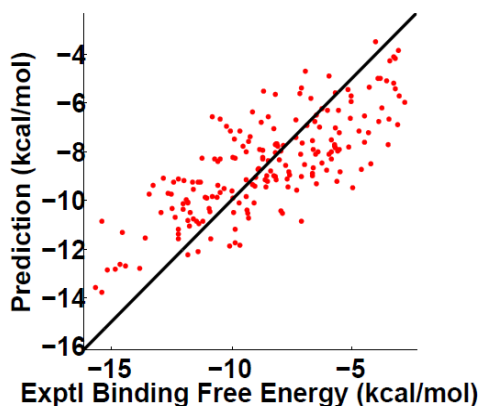


Figure 8: The correlation between experimental binding free energies and FFT-BP predictions on the PDBBind v2015 core set ($N = 195$). The RMSE and Pearson correlation coefficient are 1.92 kcal/mol and 0.78, respectively.

5 nearest neighbors and 15 features are used for the prediction.

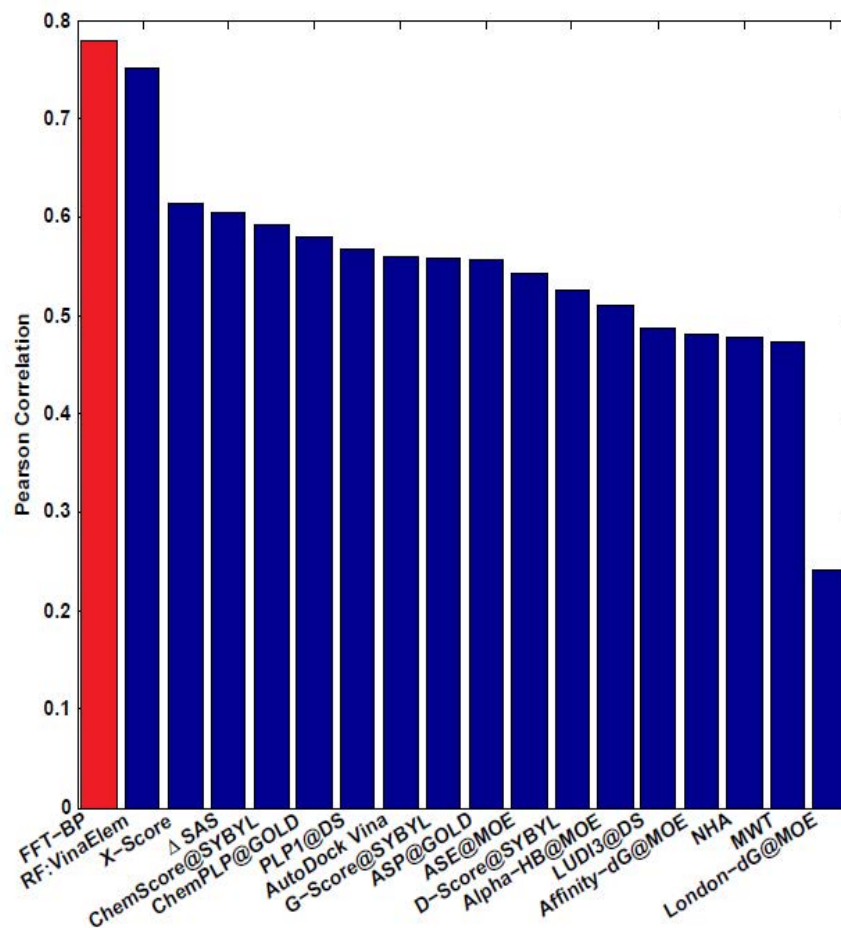
Figure 8 plots the correlation between experimental binding free energies and FFT-BP predictions on the PDBBind v2015 core set ($N = 195$). Compared to the earlier two blind predictions, the prediction on this set is more accurate. However, similar to the behavior in two other test sets, the present prediction is biased. This issue will be studied in our future work. Note that PDBBind v2015 core set is the same as the PDBBind v2013 core set, which has many test results.^{50,51} For a comparison, we plot the performance of our scoring function against several existing famous scoring functions,^{50,51} as illustrated in Fig. 9.

IV Concluding remarks

In this work, we propose a new scoring function, feature functional theory - binding predictor (FFT-BP). FFT-BP is constructed based on three fundamental assumptions, namely, representability, feature-function relationship, and similarity assumptions. A validation set of 1322 complexes, two training sets with 3589 complexes (PDBBind v2015 refined set) and 1085 complexes (PDBBind v2007 refined set), and three test sets with 100, 195 and 195 complexes are considered in the present work to

Table 8: The prediction RMSEs (kcal/mol) for the PDBBind v2015 core set ($N = 195$) with different numbers of nearest neighbors and top features.

Number of nearest neighbors	Number of top features									
	5	10	15	20	25	30	35	40	45	50
1	1.95	1.95	1.95	1.95	1.95	1.95	1.95	1.95	1.95	1.95
2	1.95	1.94	1.95	1.95	1.95	1.95	1.95	1.95	1.95	1.96
3	1.94	1.94	1.95	1.95	1.95	1.95	1.95	1.95	1.95	1.95
4	1.94	1.94	1.93	1.93	1.94	1.94	1.94	1.94	1.95	1.95
5	1.95	1.95	1.92	1.94	1.95	1.95	1.96	1.95	1.95	1.95
6	1.95	1.95	1.95	1.95	1.96	1.96	1.95	1.96	1.95	1.94
7	1.95	1.93	1.93	1.94	1.95	1.97	1.95	1.95	1.95	1.95
8	1.95	1.95	1.95	1.96	1.96	1.97	1.97	1.96	1.95	1.95
9	1.94	1.94	1.94	1.94	1.94	1.95	1.95	1.94	1.94	1.94
10	1.95	1.95	1.95	1.95	1.95	1.94	1.94	1.94	1.94	1.94

Figure 9: Performance comparison between different scoring functions on the PDBBind v2013 core set ($N = 195$). The performances of the other scoring function are adopted from the literature.^{50,51}

validate the proposed method, explore its utility, demonstrate its performance and reveal its deficiency. Extensive numerical experiments indicate that FFT-BP delivers some of the most accurate blind predictions in the field with the root-mean-square error being around 2 kcal/mol and Pearson correlation coefficient being around 0.76.

A major advantage of FFT-BP is that it extracts microscopic features from conventional implicit solvent models so that the validity of these physical models for binding analysis and prediction can be systematically examined. Consequently, the proposed FFT-BP can be improved via the improvement of our understanding on physical models. Another advantage of FFT-BP is that it provides a framework to systematically incorporate and continuously absorb advanced machine learning algorithms to improve its predictive power. The other advantage of FFT-BP is that it becomes more and more accurate as the existing binding database becomes larger and larger.

This work is our first attempt in exploring the mathematical modeling of the protein-ligand binding affinity. Our model can be further improved in several aspects. First, we have employed a very crude force field parametrized of the Poisson model. More accurate Poisson-Boltzmann (PB) modeling, such as polarizable PB model, and feature extraction from more accurate quantum mechanics/molecular mechanics (QM/MM) models will improve the present FFT-BP. Additionally, we employ the MART algorithm for the molecules ranking. More sophisticated machine learning algorithms, such as deep learning, can

potentially improve FFT-BP prediction, and eliminate the current prediction bias in test sets. Finally, a deficiency of the current model is that it neglects the metal effect on protein-ligand binding affinity. The incorporation of this effect into our model is under our investigation.

Acknowledgments

This work was supported in part by NSF Grant IIS- 1302285 and MSU Center for Mathematical Molecular Biosciences Initiative. We thank Emil Alexov, Michael Gilson, Ray Luo, Wei Yang and John Zheng for useful discussions.

References

- [1] CERIOUS2 LigandFit User Manual; Accelrys, Inc.: San Deigo, CA. pages 3–48, 2000.
- [2] S. Agarwal, D. Dugar, and S. Sengupta. Ranking chemical structure for drug discovery: A new machine learning approach. *Journal of Chemical Information and Model*, 50:716–731, 2010.
- [3] H. M. Ashtawy and N. R. Mahapatra. A comparative assessment of ranking accuracies of conventional and machine-learning-based scoring functions for protein-ligand binding affinity prediction. *IEEE/ACM Transactions on computational biology and bioinformatics*, 9(5):1301–1313, 2012.
- [4] P. J. Ballester. Machine learning scoring functions based on random forest and support vector regression. *Proceedings of the 7th IAPR international conference on Pattern Recognition in Bioinformatics*, pages 14–25, 2012.
- [5] P. J. Ballester and J. B. O. Mitchell. A machine learning approach to predicting protein-ligand binding affinity with applications to molecular docking. *Bioinformatics*, 26(9):1169–1175, 2010.
- [6] P. J. Ballester, A. Schreyer, and L. B. Tom. Does a more precise chemical description of protein-ligand complexes lead to more accurate prediction of binding affinity? *Journal of Chemical Information and Model*, 54:944–955, 2014.
- [7] B. Baum, L. Muley, M. Smolinski, A. Heine, D. Hangauer, and G. Klebe. Non-additivity of functional group contributions in protein-ligand binding: a comprehensive study by crystallography and isothermal titration calorimetry. *J. Mol. Bio*, 397(4):1042–1054, 2010.
- [8] J. R. Bock and D. A. Gough. A new method to estimate ligand-receptor energetics. *Molecular and Cellular Proteomics*, 1(11):904–910, 2002.
- [9] H. J. Bohm. The development of a simple empirical scoring function to estimate the binding constant for a protein-ligand complex of known three-dimensional structure. *Journal of Computer-Aided Molecular Design*, 8:234–256, 1994.
- [10] C. J. Burges. From RankNet to LambdaRank to LambdaMART: An overview. *Microsoft Research Technical Report*, 82, 2010.
- [11] B. D. Bursulaya, M. Totrov, R. Abagyan, and C. L. Brooks. Comparative study of several algorithms for flexible ligand docking. *Journal of Computer-Aided Molecular Design*, 17:755–763, 2003.
- [12] Y. Cao and L. Li. Improved protein-ligand binding affinity prediction by using a curvature-dependent surface-area model. *Bioinformatics*, 30(12):1674–1680, 2014.
- [13] Z. Cao, T. Qin, T. Y. Liu, M. F. Tsai, and F. Li. Learning to rank: From pairwise approach to listwise approach. *ICML*, 2007.
- [14] D. A. Case, J. T. Berryman, R. M. Betz, D. S. Cerutti, T. E. C. III, T. A. Darden, R. E. Duke, T. J. Giese, H. Gohlke, A. W. Goetz, N. Homeyer, S. Izadi, P. Janowski, J. Kaus, A. Kovalenko, T. S. Lee, S. LeGrand, P. Li, T. Luchko, R. Luo, B. Madej, K. M. Merz, G. Monard, P. Needham, H. Nguyen, H. T. Nguyen, I. Omelyan, A. Onufriev, D. R. Roe, A. Roitberg, R. Salomon-Ferrer, C. L. Simmerling, W. Smith, J. Swails, R. C. Walker, J. Wang, R. Wolf, X. Wu, D. M. York, and P. A. Kollman. Amber 2015. *University of California, San Francisco*, 2015.
- [15] D. Chen, Z. Chen, C. Chen, W. H. Geng, and G. W. Wei. MIBPB: A software package for electrostatic analysis. *J. Comput. Chem.*, 32:657 – 670, 2011.
- [16] Z. Chen, N. A. Baker, and G. W. Wei. Differential geometry based solvation models I: Eulerian formulation. *J. Comput. Phys.*, 229:8231–8258, 2010.
- [17] Z. Chen, S. Zhao, J. Chun, D. G. Thomas, N. A. Baker, P. B. Bates, and G. W. Wei. Variational approach for nonpolar solvation analysis. *Journal of Chemical Physics*, 137(084101), 2012.
- [18] T. Cheng, X. Li, Y. Li, Z. Liu, and R. Wang. Comparative assesment of scoring functions on a diverse test set. *J. Chem. Inf. Model.*, 49:1079–1093, 2009.
- [19] N. Choudhury and B. M. Pettitt. On the mechanism of hydrophobic association of nanoscopic solutes. *Journal of the American Chemical Society*, 127(10):3556–3567, 2005.

- [20] R. L. DesJarlais, R. P. Sheridan, J. S. Dixon, I. D. Kuntz, and R. Venkataraghavan. Docking flexible ligands to macromolecular receptors by molecular shape. *J. Med. Chem.*, 29:2149–2153, 1986.
- [21] M. D. Eldridge, C. W. Murray, T. R. Auton, G. V. Paolini, and R. P. Mee. Empirical scoring functions: I. the development of a fast empirical scoring function to estimate the binding affinity of ligands in receptor complexes. *J. Comput. Aided Mol. Des.*, 11:425–445, 1997.
- [22] J. H. Friedman. Greedy function approximation: a gradient boosting machine. *Annals of statistics*, pages 1189–1232, 2001.
- [23] R. A. Friesner, J. L. Banks, R. B. Murphy, T. A. Halgren, J. J. Klicic, D. T. Mainz, M. P. Repasky, E. H. Knoll, M. Shelley, J. K. P. JK, D. E. Shaw, P. Francis, and P. S. Shenkin. Glide: a new approach for rapid, accurate docking and scoring. 1. method and assessment of docking accuracy. *J. Med. Chem.*, 47:1739, 2004.
- [24] E. Gallicchio and R. M. Levy. AGBNP: An analytic implicit solvent model suitable for molecular dynamics simulations and high-resolution modeling. *Journal of Computational Chemistry*, 25(4):479–499, 2004.
- [25] E. Gallicchio, L. Y. Zhang, and R. M. Levy. The SGB/NP hydration free energy model based on the surface generalized Born solvent reaction field and novel nonpolar hydration free energy estimators. *Journal of Computational Chemistry*, 23(5):517–29, 2002.
- [26] D. Gehlhaar, G. Verkhivker, P. Rejto, C. Sherman, D. Fogel, L. Fogel, and S. Freer. Molecular recognition of the inhibitor AG-1343 by HIV-1 protease: conformationally flexible docking by evolutionary programming. *Chem Biol.*, 2(5):317–324, 1995.
- [27] W. Geng, S. Yu, and G. W. Wei. Treatment of charge singularities in implicit solvent models. *Journal of Chemical Physics*, 127:114106, 2007.
- [28] M. K. Gilson, M. E. Davis, B. A. Luty, and J. A. McCammon. Computation of electrostatic forces on solvated molecules using the Poisson-Boltzmann equation. *Journal of Physical Chemistry*, 97(14):3591–3600, 1993.
- [29] M. K. Gilson and H. X. Zhou. Calculation of protein-ligand binding affinities. *Annual Review of Biophysics and Biomolecular Structur*, 36:21–42, 2007.
- [30] H. Gohlke, M. Hendlich, and G. Klebe. Knowledge-based scoring function to predict protein-ligand interactions. *J Mol Biol.*, 295(2):337–356, 2000.
- [31] D. S. Goodsell and A. J. Olson. Automated docking of substrates to proteins by simulated annealing. *Protein Struct. Funct. Genet.*, 8:195–202, 1990.
- [32] P. A. Greenidge, C. Kramer, J.-C. Mozziconacci, and R. M. Wolf. MM/GBSA binding energy prediction on the PDBBind data set: Successes, failures, and directions for further improvement. *Journal of Chemical Information and Model*, 53:201–209, 2013.
- [33] B. Honig and A. Nicholls. Classical electrostatics in biology and chemistry. *Science*, 268(5214):1144–9, 1995.
- [34] S. Y. Huang and X. Zou. An iterative knowledge-based scoring function to predict protein-ligand interactions: I. derivation of interaction potentials. *J. Comput. Chem.*, 27:1865–1875, 2006.
- [35] S.-Y. Huang and X. Zou. Inclusion of solvation and entropy in the knowledge-based scoring function for proteinligand interactions. *J. Chem. Inf. Model.*, 50(2):262–273, 2010.
- [36] A. Jakalian, D. B. Jack, and C. I. Bayly. Fast, efficient generation of high-quality atomic charges. AM1-BCC model: II. parameterization and validation. *Journal of Computational Chemistry*, 23(16):1623–1641, 2002.
- [37] T. Joachims. Optimizing search engines using clickthrough data. *Proceedings of the ACM Conference on Knowledge Discovery and Data Mining (KDD)*, 2002.
- [38] T. Joachims. Training linear SVMs in linear time. *Proceedings of the ACM Conference on Knowledge Discovery and Data Mining (KDD)*, 2006.
- [39] G. Jones, P. Willett, R. C. Glen, A. R. Leach, and R. Taylor. Development and validation of a genetic algorithm for flexible docking. *Journal of Molecular Biology*, 267(3):727–748, 1997.
- [40] W. L. Jorgensen. Rusting of the lock and key model for protein-ligand binding. *Science*, 254:954–955, 1991.

- [41] W. L. Jorgensen and J. Tirado-Rives. The OPLS optimized potentials for liquid simulations] potential functions for proteins, energy minimizations for crystals of cyclic peptides and crambin. *J. Am. Chem. Soc.*, 110(6):1657–1666, 1988.
- [42] S. L. Kinnings, N. Liu, P. J. Tonge, R. M. Jackson, L. Xie, and P. E. Bourne. A machine learning based method to improve docking scoring functions and its application to drug repurposing. *Journal of Chemical Information and Model*, 51(2):408–419, 2011.
- [43] P. A. Kollman, I. Massova, C. Reyes, B. Kuhn, S. Huo, L. Chong, M. Lee, T. Lee, Y. Duan, W. Wang, O. Donini, P. Cieplak, J. Srinivasan, D. A. Case, and I. Cheatham, T. E. Calculating structures and free energies of complex molecules: combining molecular mechanics and continuum models. *Accounts of Chemical Research*, 33(12):889–97, 2000.
- [44] I. D. Kuntz, J. M. Blaney, S. J. Oatley, R. Langridge, and T. E. Ferrin. A geometric approach to macromolecule-ligand interactions. *J. Mol. Biol.*, 161:269–288, 1982.
- [45] T.-M. Kuo, C.-P. Lee, and C.-J. Lin. Large-scale kernel RankSVM. *SIAM International Conference on Data Mining*, 2014.
- [46] A. R. Leach, B. K. Shoichet, and C. E. Peishoff. Prediction of protein-ligand interactions. docking and scoring: Successes and gaps. *J. Med. Chem.*, 49:5851–5855, 2006.
- [47] G.-B. Li, L.-L. Yang, W.-J. Wang, L.-L. Li, and S.-Y. Yang. ID-Score: A new empirical scoring function based on a comprehensive set of descriptors related to proteinligand interactions. *J. Chem. Inf. Model.*, 53(3):592–600, 2013.
- [48] H. Li, K. Leung, P. Ballester, and M. H. Wong. iStar: A web platform for large-scale protein-ligand docking. *Plos One*, 9(1), 2014.
- [49] H. Li, K.-S. Leung, M. Wong, and P. J. Ballester. Substituting random forest for multiple linear regression improves binding affinity prediction of scoring functions: Cyscore as a case study. *BMC Bioinformatics*, 15(291), 2014.
- [50] H. Li, K.-S. Leung, M.-H. Wong, and P. J. Ballester. Low-Quality Structural and Interaction Data Improves Binding Affinity Prediction via Random Forest. *Molecules*, 20:10947–10962, 2015.
- [51] Y. Li, L. Han, Z. Liu, and R. Wang. Comparative assessment of scoring functions on an updated benchmark: 2. evaluation methods and general results. *Journal of chemical information and modeling*, 54(6):1717–1736, 2014.
- [52] B. Liu, B. Wang, R. Zhao, Y. Tong, and G. W. Wei. ESES: software for Eulerian solvent excluded surface. *Journal of Computational Chemistry*, 38:446–466, 2017.
- [53] J. Liu and R. Wang. Clasification of current scoring functions. *Journal of Chemical Information and Model*, 55(3):475–482, 2015.
- [54] Z. Liu, Y. Li, L. Han, J. Liu, Z. Zhao, W. Nie, Y. Liu, and R. Wang. PDB-wide collection of binding data: current status of the PDBbind database. *Bioinformatics*, 31(3):405–412, 2015.
- [55] K. Lum, D. Chandler, and J. D. Weeks. Hydrophobicity at small and large length scales. *Journal of Physical Chemistry B*, 103(22):4570–7, 1999.
- [56] J. MacKerell, A. D., D. Bashford, M. Bellot, J. Dunbrack, R. L., J. D. Evanseck, M. J. Field, S. Fischer, J. Gao, H. Guo, S. Ha, D. Joseph-McCarthy, L. Kuchnir, K. Kuczera, F. T. K. Lau, C. Mattos, S. Michnick, T. Ngo, D. T. Nguyen, B. Prodrom, I. Reiher, W. E., B. Roux, M. Schlenkrich, J. C. Smith, R. Stote, J. Straub, M. Watanabe, J. Wiorkiewicz-Kuczera, D. Yin, and M. Karplus. All-atom empirical potential for molecular modeling and dynamics studies of proteins. *Journal of Physical Chemistry B*, 102(18):3586–3616, 1998.
- [57] I. Massova and P. A. Kollman. Combined molecular mechanical and continuum solvent approach (MM-PBSA/GBSA) to predict ligand binding. *Perspectives in drug discovery and design*, 18(1):113–135, 2000.
- [58] E. C. Meng, B. K. Shoichet, and I. D. Kuntz. Automated docking with grid-based energy evaluation. *Journal of Computational Chemistry*, 13:505–524, 1992.
- [59] G. M. Morris, D. S. Goodsell, R. S. Halliday, R. Huey, W. E. Hart, R. K. Belew, and A. J. Olson. Automated docking using a lamarckian genetic algorithm and an empirical binding free energy function. *Journal of Computational Chemistry*, 19:1639–62, 1998.
- [60] I. Muegge and Y. Martin. A general and fast scoring function for protein-ligand interactions: a simplified potential approach. *J Med Chem.*, 42(5):791–804, 1999.

- [61] D. D. Nguyen, B. Wang, and G. W. Wei. Accurate, robust and reliable calculations of Poisson-Boltzmann binding energies. *Journal of Computational Chemistry*, 38, 2017.
- [62] F. N. Novikov, A. A. Zeifman, O. V. Stroganov, V. S. Stroylov, V. Kulkov, and G. G. Chilov. CSAR Scoring challenge reveals the need for new concepts in estimating protein-ligand binding affinity. *Journal of Chemical Information and Model*, 51:2090–2096, 2011.
- [63] M. H. M. Olsson, C. R. Sondergaard, M. Rostkowski, and J. H. Jensen. PROPKA3: consistent treatment of internal and surface residues in empirical pka predictions. *J. Chem. Theory Comput.*, 7(2):525–537, 2011.
- [64] A. R. Ortiz, M. T. Pisabarro, F. Gago, and R. C. Wade. Prediction of drug binding affinities by comparative binding energy analysis. *J. Med. Chem*, 38:2681–2691, 1995.
- [65] R. A. Pierotti. A scaled particle theory of aqueous and nonaqueous solutions. *Chemical Reviews*, 76(6):717–726, 1976.
- [66] J. W. Ponder, C. J. Wu, P. Y. Ren, V. S. Pande, J. D. Chodera, M. J. Schnieders, I. Haque, D. L. Mobley, D. S. Lambrecht, R. A. DiStasio, M. Head-Gordon, G. N. I. Clark, M. E. Johnson, and T. Head-Gordon. Current status of the amoeba polarizable force field. *J. Phys. Chem. B*, 114:2549 – 2564, 2010.
- [67] M. Rarey, B. Kramer, T. Lengauer, and G. Klebe. A fast flexible docking method using an incremental construction algorithm. *J Mol Biol.*, 261(3):470–489, 1996.
- [68] W. Rocchia, E. Alexov, and B. Honig. Extending the applicability of the nonlinear poisson-boltzmann equation: Multiple dielectric constants and multivalent ions. *J. Phys. Chem.*, 105:6507–6514, 2001.
- [69] M. Rostkowski, M. H. Olsson, C. R. Sondergaard, and J. H. Jensen. Graphical analysis of pH-dependent properties of proteins predicted using PROPKA. *BMC Structural Biology*, 11(6), 2011.
- [70] G. M. Sastry, M. Adzhigirey, T. Day, R. Annabhimoju, and W. Sherman. Protein and ligand preparation: parameters, protocols, and influence on virtual screening enrichments. *J. Comput. Aid. Mol. Des.*, 27:221–234, 2013.
- [71] B. Schichet. Virtual screening of chemical libraries. *Nature*, 432(7019):862–865, 2004.
- [72] K. A. Sharp and B. Honig. Calculating total electrostatic energies with the nonlinear Poisson-Boltzmann equation. *Journal of Physical Chemistry*, 94:7684–7692, 1990.
- [73] K. A. Sharp and B. Honig. Electrostatic interactions in macromolecules - theory and applications. *Annual Review of Biophysics and Biophysical Chemistry*, 19:301–332, 1990.
- [74] F. H. Stillinger. Structure in aqueous solutions of nonpolar solutes from the standpoint of scaled-particle theory. *J. Solution Chem.*, 2:141 – 158, 1973.
- [75] P.-C. Su, C.-C. Tsai, S. Mehboob, K. E. Heveber, and M. E. Johnson. Comparison of radii sets, entropy, qm methods, and sampling on MM-PBSA, MM-GBSA, and QM/MM-GBSA ligand binding energies of f. tularensis enoyl-acp reductase (fabI). *Journal of Computational Chemistry*, 36:1859–1873, 2015.
- [76] O. Trott and A. J. Olson. AutoDock Vina: improving the speed and accuracy of docking with a new scoring function, efficient optimization, and multithreading. *J Computat Chem*, 31(2):455–461, 2010.
- [77] H. Velec, H. Gohlke, and G. Klebe. DrugScore (CSD)-knowledge-based scoring function derived from small molecule crystal data with superior recognition rate of near-native ligand poses and better affinity prediction. *J Med Chem.*, 48(20):6296–303, 2005.
- [78] H. F. G. Velec, H. Gohlke, and G. Klebe. Knowledge-based scoring function derived from small molecule crystal data with superior recognition rate of near-native ligand poses and better affinity prediction. *J. Med. Chem*, 48:6296–6303, 2005.
- [79] G. Verkhivker, K. Appelt, S. T. Freer, and J. E. Villafranca. Empirical free energy calculations of ligand-protein crystallographic complexes. i. knowledge based ligand-protein interaction potentials applied to the prediction of human immunodeficiency virus protease binding affinity. *Protein Eng*, 8:677–691, 1995.
- [80] J. A. Wagoner and N. A. Baker. Assessing implicit models for nonpolar mean solvation forces: the importance of dispersion and volume terms. *Proceedings of the National Academy of Sciences of the United States of America*, 103(22):8331–6, 2006.
- [81] N. Wale and G. Karypis. Target fishing for chemical compounds using target-ligand activity data and ranking based methods. *Journal of Chemical Information and Model*, 49(10):2190–201, 2009.

- [82] B. Wang, C. Wang, and G. W. Wei. Learning to rank for solvation free energy prediction. *Preprint*, 2016.
- [83] B. Wang and G. W. Wei. Parameter optimization in differential geometry based solvation models. *Journal Chemical Physics*, 143:134119, 2015.
- [84] J. Wang, R. M. Wolf, J. W. Caldwell, P. A. Kollman, and D. A. Case. Development and testing of a general AMBER force field. *Journal of Computational Chemistry*, 25(9):1157–74, 2004.
- [85] R. Wang, L. Lai, and S. Wang. Further development and validation of empirical scoring functions for structure based binding affinity prediction. *J. Comput. Aided. Mol. Des*, 16:11–26, 2002.
- [86] R. Wang, Y. Lu, and S. Wang. Comparative evaluation of 11 scoring functions for molecular docking. *J. Med. Chem.*, 46:2287–2303, 2003.
- [87] A. M. Wassermann, H. Geppert, and J. R. Bajorath. Searching for target-selective compounds using different combinations of multiclass support vector machine ranking methods, kernel functions, and fingerprint descriptors. *Journal of Chemical Information and Model*, 49(3):582–92, 2009.
- [88] G. W. Wei. Differential geometry based multiscale models. *Bulletin of Mathematical Biology*, 72:1562 – 1622, 2010.
- [89] S. J. Weiner, P. A. Kollman, D. T. Nguyen, and D. A. Case. An all atom force-field for simulations of proteins and nucleic-acids. *J Comp Chem*, 7(2):230–252, 1986.
- [90] S. Yin, L. Biedermannova, J. Vondrasek, and N. V. Dokholyan. Medusascoring: An accurate force field-based scoring function for virtual drug screening. *Journal of Chemical Information and Model*, 48:1656–1662, 2008.
- [91] S. N. Yu, W. H. Geng, and G. W. Wei. Treatment of geometric singularities in implicit solvent models. *Journal of Chemical Physics*, 126:244108, 2007.
- [92] C. Zhang, S. Liu, Q. Zhu, and Y. Zhou. A knowledge-based energy function for protein-ligand, protein-protein, and protein-dna complexes. *J Med Chem.*, 48(7):2325–35, 2005.
- [93] W. Zhang, L. Ji, Y. Chen, K. Tang, H. Wang, R. Zhu, W. Jia, Z. Cao, and Q. Liu. When drug discovery meets web search: Learning to rank for ligand-based virtual screening. *Journal of Cheminformatics*, 7(5), 2015.
- [94] Z. Zheng and K. M. Merz Jr. Ligand identification scoring algorithm (LISA). *Journal of Chemical Information and Model*, 51:1296–1306, 2011.
- [95] Z. Zheng and K. M. Merz Jr. Development of the knowledge-based and empirical combined scoring algorithm (KECSA) to score proteinligand interactions. *Journal of Chemical Information and Model*, 53:1073–1083, 2013.
- [96] Z. Zheng, M. N. Ucisik, and K. M. Merz Jr. The movable type method applied to proteinligand binding. *Journal of Chemical Theory and Computation*, 9:5526–5538, 2013.
- [97] H.-X. Zhou and M. K. Gilson. Theory of free energy and entropy in noncovalent binding. *Chemical reviews*, 109(9):4092–4107, 2009.
- [98] Y. C. Zhou, S. Zhao, M. Feig, and G. W. Wei. High order matched interface and boundary method for elliptic equations with discontinuous coefficients and singular sources. *J. Comput. Phys.*, 213(1):1–30, 2006.